THE UNIVERSITY OF MICHIGAN

7692-3-Q

Electromagnetic Coupling Reduction Techniques

Third Quarterly Report
15 June 1966 - 14 August 1966

By

J.A.M. Lyon, N.G. Alexopoulos, A.G. Cha
C.J. Digenis, and W.W. Parker

August 1966

Contract No. AF 33(615)-3371
Project 4357, Task 435709

Prepared for

Air Force Avionics Laboratory
United States Air Force, AFSC
Wright-Patterson AFB, Ohio 45433

FOREWORD

This report 7692-3-Q was prepared by The University of Michigan, Ann Arbor, Michigan, under the direction of Professor Ralph E. Hiatt and Professor John A. M. Lyon and on Air Force Contract AF 33(615)-3371 under Task No. 435709 of Project 4357 (U) "Electromagnetic Coupling Reduction Techniques". The work was administered under the direction of the Air Force Avionics Laboratory, Electronic Warfare Division, Research and Technology Division, Wright-Patterson Air Force Base Ohio. The Task Engineer was Mr. Olin E. Horton, the Project Engineer Mr. Herbert Bartman.

This report covers the period 15 June 1966 through 14 August 1966.

TABLE OF CONTENTS

LIST OF FIGURES

LIST OF FIGURES
(continued)

ABSTRACT

During this report period, additional studies were made on horns and slots surrounded by absorbing material. New designs were used which permitted all of the absorbing material to be flush with the conducting surface. Swept frequency methods were used in obtaining values for the increased isolation over a considerable range of frequency.

Studies were made on the isolation of two antennas through the use of chokes. A slot antenna was constructed surrounded by four chokes in the form of circumferential trenches. For two systems, each equipped with such circumferential chokes, an additional 22 db of isolation was obtained.

Additional studies were made on the use of corrugations to increase isolation. The corrugations described here are not of an optimized design and do not use absorber material as has been planned for the future.

Simple parasitic antenna elements, such as slots as reflectors, have been used to improve system isolation. The improvement is rather small, being limited to about 7 db.

Considerable effort has been utilized on developing an RF bridge to improve isolation by cancellation of the unwanted signal. Results have been encouraging but work remains to adapt this method to a wider bandwidth.

I

INTRODUCTION

Several of the items covered during this report are continuations of studies commenced and partially described in the previous quarterly report. Emphasis has been placed upon obtaining as much bandwidth as possible for decoupling for each of the decoupling methods studied. For convenience the measurements were often made at the X-band frequencies but none of the decoupling methods is limited to that frequency band.

The initial experimentation using absorber was sufficiently encouraging so that newly designed sectoral horns and slot antennas were used in connection with absorber. The absorber studied was Eccosorb MF-124. Systems, each of which used an E-sectoral horn, were found to have an increased isolation of 18 db. Two systems, each using a slot antenna, with surrounding absorber as studied here, show an increase of 13 db isolation. In both instances, the increased isolation can be obtained over the entire X band.

A slot antenna was designed with four circumferential slots surrounding the driven slot. Two systems, each having such a connected slot, with surrounding circumferential chokes or trenches, would have increased isolation from one system to another of the order of 22 db over 0.5 GHz within the X-band of frequencies.

Two ordinary slot antennas were tested for increased isolation from one to another by the insertion of corrugations between the slots. The tops of the corrugations were flush mounted with the conducting surface. The systems were then found to be isolated by an increase of 5 db over the entire X-band. The work on corrugations is by no means complete; it is expected that corrugations of different depths

and with different loading materials in the trenches will be used.

Some favorable results were obtained through the use of parasitic antennas. In the experimental case explored, a slot antenna was considered with a second parasitic slot in back of it. The parasitic slot acted as a reflector. If the transmission system has a slot radiator with a slot reflector and likewise the receiving system has a slot antenna with a slot reflector, it is found that the isolation increase between the two systems using these parasitics is approximately 7 db. Additional parasitic elements used as directors had very little effect as far as increase of isolation. The isolation increase was good for a 2.5 GHz bandwidth for X-band operation.

Another method of isolation explored, at least in a preliminary way, was through the use of a bridge link or cancellation method. The principle of the bridge link is to make a second path from transmitting antenna to receiving antenna which will deposit a signal at the receiving antenna which will just cancel the undesired signal from the transmitting antenna. Proceeding in this fashion, a bridge method is described in the report, wherein 15 db of increased isolation is obtained for a bandwidth of 1.5 GHz for X-band operation. This seemed to be very promising. Extensions of the bridge method, including filtering, are described later in the report.

II

EXPERIMENTAL STUDIES

2.1 Introductory Remarks

In studying methods for achieving reduction of the electromagnetic coupling between two antennas mounted on a common ground plane the following information in terms of charts or graphs is considered to be necessary and sufficient in most cases: maximum gain versus frequency, E- and H-plane radiation patterns at one or more frequencies, E- and H-plane coupling versus frequency, and E- and H-plane coupling versus receiving antenna orientation at one or more frequencies.

It should be pointed out that the term "gain" is used with the meaning (Kraus, 1950) "directivity times efficiency". This clarification becomes necessary because some authors use the term gain with the meaning of directivity. When absorbing materials are used in the vicinity of the aperture of a microwave antenna with the purpose of reducing the interference to a nearby antenna it has been observed (Lyon, et al, 1966) that in some cases although the antenna directivity is not seriously affected, the antenna efficiency is reduced resulting in considerable loss of gain. Since any decoupling method resulting in gain reduction is not considered an acceptable solution the variation of gain must always be studied. The types of antennas considered radiate mainly broadside to the conducting ground plane. Therefore, the variation of gain was studied in this direction.

Coupling from one antenna to another when the receiving antenna is rotated has already been presented (Lyon, et al, 1966)

Since for aerodynamic reasons all antennas on aircraft or aerospace vehicles are flush-mounted any coupling reduction technique would not be acceptable unless if it avoids any protrusions above the ground plane. All techniques presented in this report meet this requirement.

One important aspect of decoupling is broadbanding. A swept frequency technique was used to give faster and more complete information on the dependence of coupling upon frequency than the previously used point-by-point method. The circuit, in block diagram form, is shown on Fig. 2-1: When sweeping the frequency one has to abandon the slide-screw tuners used in the point-by-point method to match the aperture with the waveguide impedance. By using the tuning devices, the coupling obtained represents the most pessimistic estimate. However, the elimination of the tuners was not found to be responsible for more than approximately 0.5 db change in the coupling level; besides the new system most probably represents a more realistic case in view of the applications.

When measuring coupling, flanges A and B (Fig. 2-1) mate to establish the reference level shown on all swept-frequency coupling charts. In measuring variation of gain versus frequency a standard 2" x 2" horn was used as a receiver (in the far-field of the antenna). The gain patterns indicate only the relative level, i.e. whether a particular decoupling method tends to increase or decrease the gain of the original antenna.

2.2 Decoupling of Two Antennas by Means of Absorbing Materials

2.2.1 E-Sectoral Horns

A new arrangement was designed and manufactured to permit the aperture of an E-Sectoral Horn to be surrounded by absorbing material and at the same time result in a flush-mounted structure (see Fig. 2-2). The absorber used is Emerson and Cuming's Eccosorb MF-124 for which the manufacturer specifies an average value of attenuation 69 db/cm (at 10 GHz).

The variation of gain with frequency is shown in Fig. 2-3. The comparison with the control horn shows a small loss in antenna gain of the order of 0.5 db. Radiation patterns for three different frequencies are shown in Fig. 2-4. The pattern at 10 GHz, where the strongest coupling has been observed, shows that the

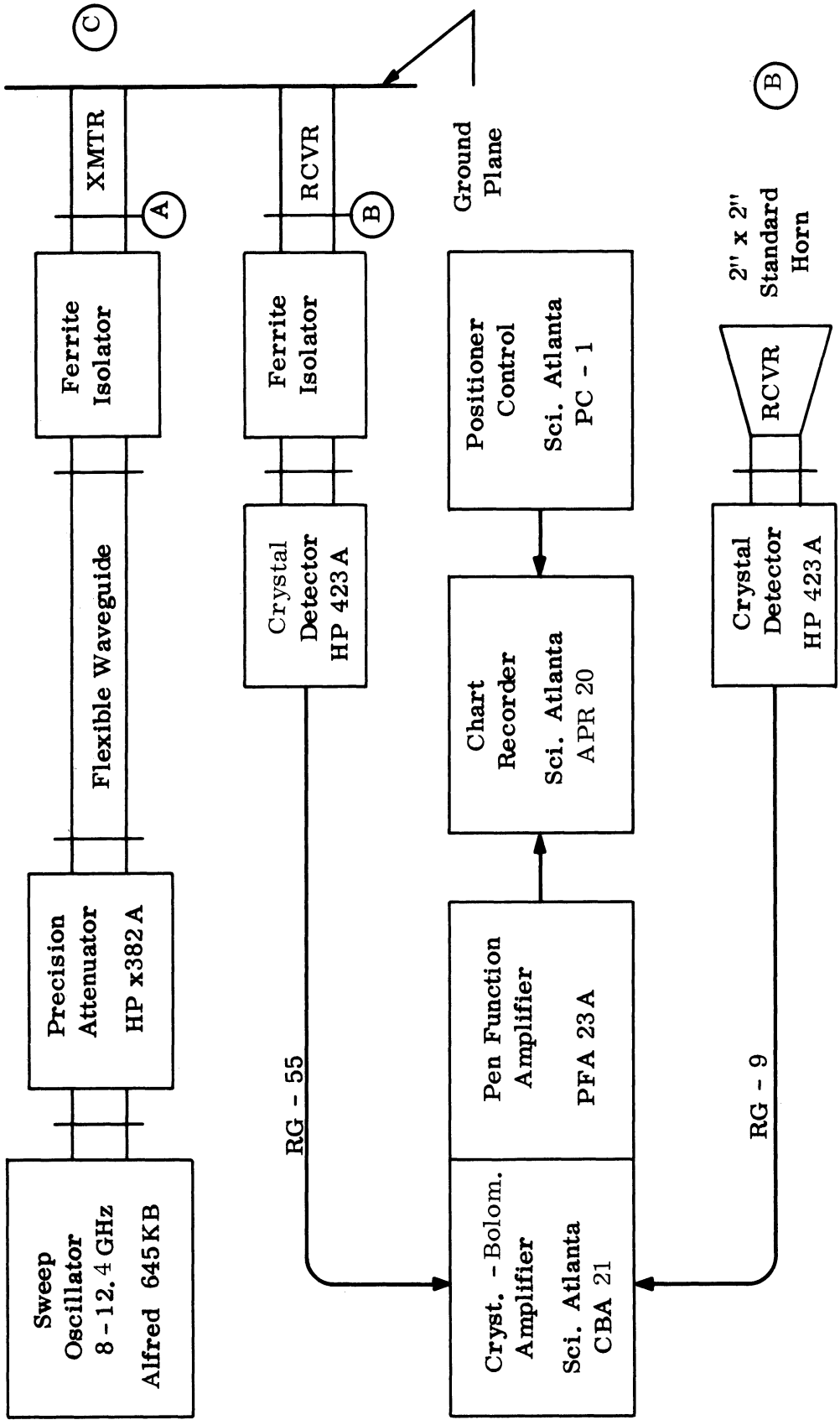

FIG. 2-1: BLOCK DIAGRAM OF SWEPT FREQUENCY CIRCUIT.

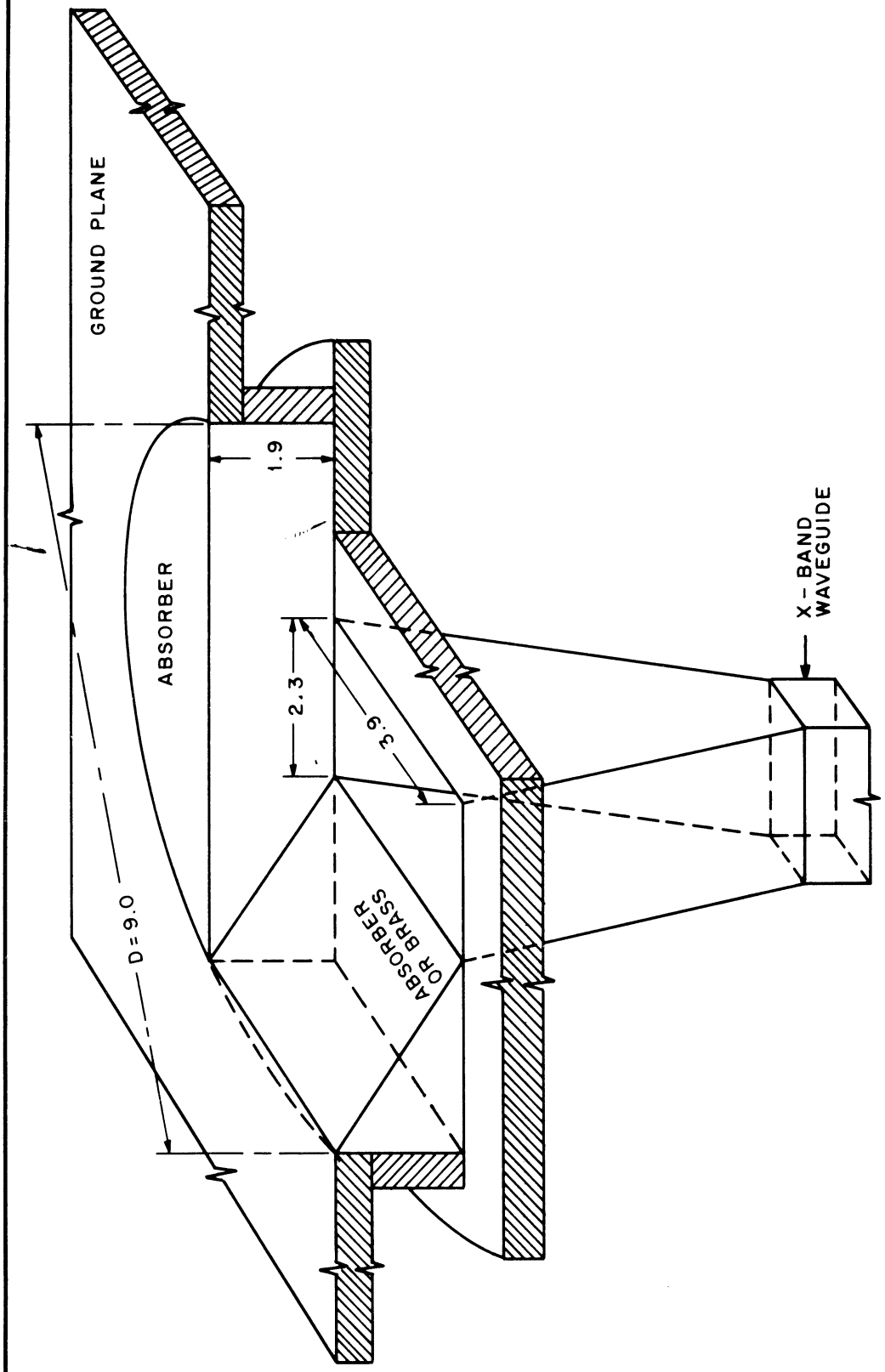

FIG. 2-2: RECESSED E-SECTORAL HORN AND ABSORBER GEOMETRY
(Dimensions in cm)

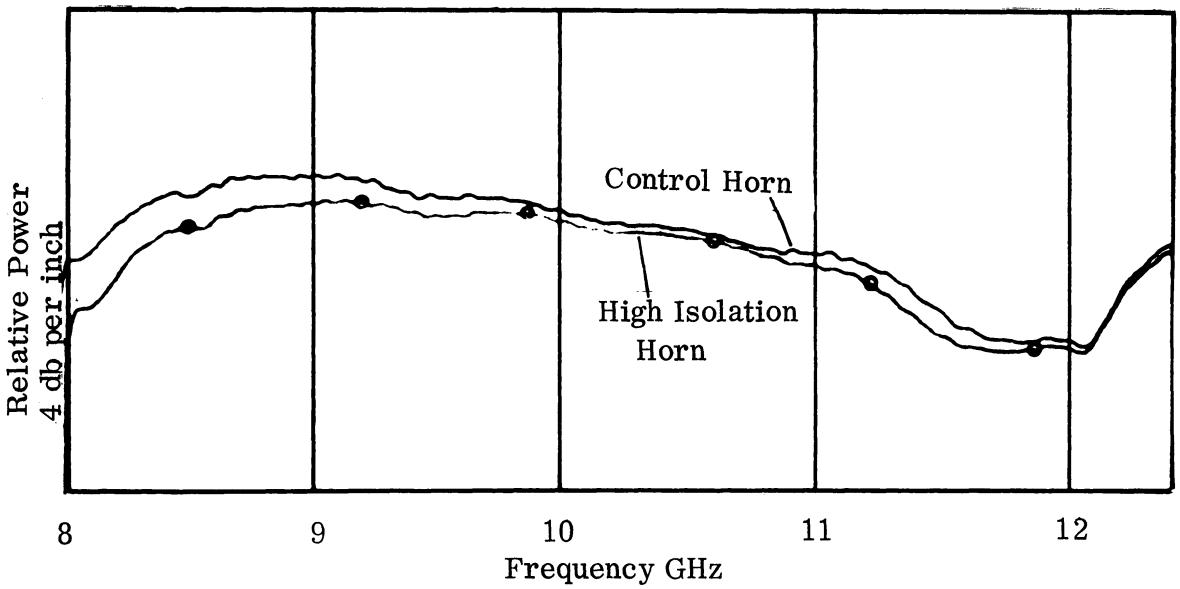

FIG. 2-3: MAXIMUM GAIN VERSUS FREQUENCY FOR E-SECTORAL HORNS

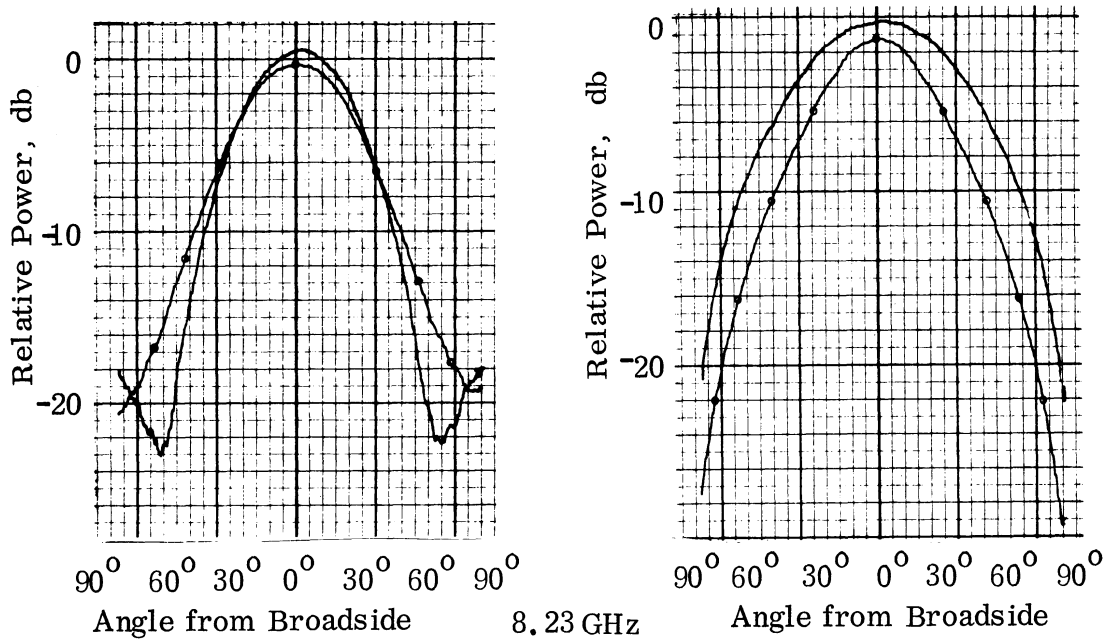

(a) E-Plane (b) H-Plane

FIG. 2-4: E- AND H-PLANE RADIATION PATTERNS OF E-SECTORAL HORNS, (——) Control Horn; (—o—) Isolation Horn.

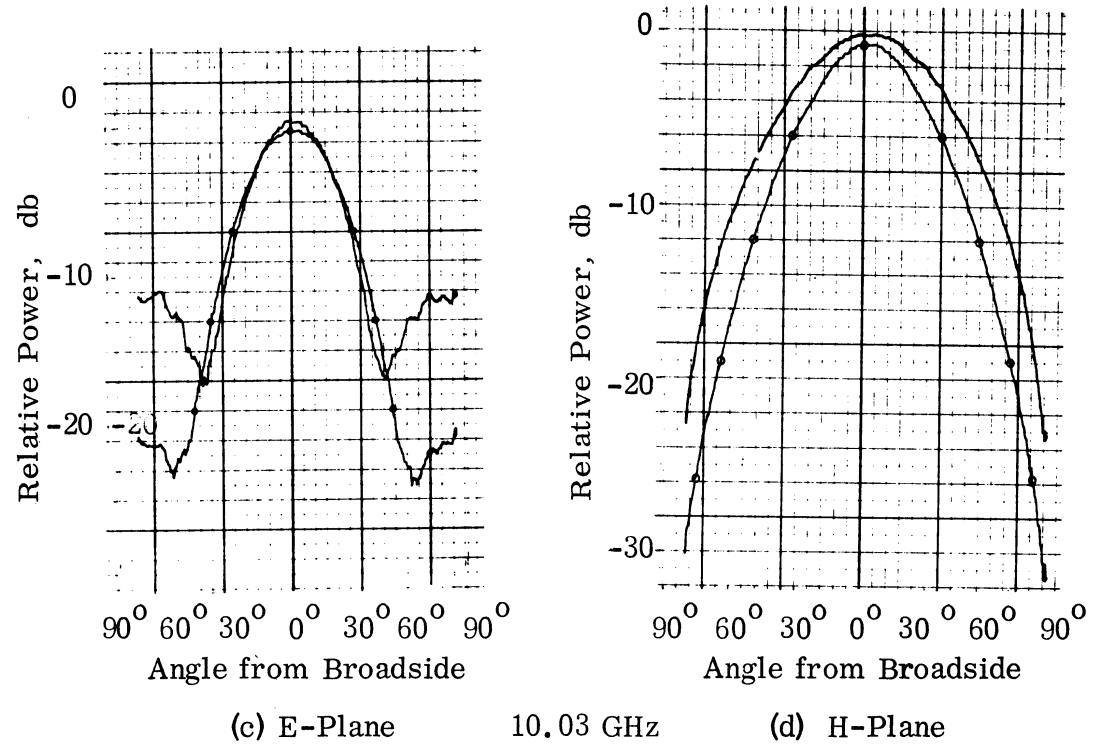

FIG. 2-4: E- AND H-PLANE RADIATION PATTERNS OF E-SECTORAL HORNS; (—) Control Horn; (—o—) Isolation Horn.

presence of the absorber leaves the main lobe practically unchanged, while it reduces the side lobes by approximately 9 db.

Coupling patterns versus frequency for both the modified (high isolation) horn and the control horn (i.e. a flush-mounted horn with aperture 2.3 cm x 3.9 cm) are shown in Fig. 2-5. It should be noted that the high-isolation modification was applied only to the transmitting horn, i.e., the same receiver was used for all the coupling patterns of Fig. 2-5. Therefore, according to the symmetry argument, twice as much decoupling should be expected if both transmitter and receiver were modified according to Fig. 2-2. Thus for E-plane coupling the increase in isolation is approximately 18 db while for H-plane, it is 15 db.

Since the swept-frequency generator output varied with frequency (by $\pm$ 0.75 db) constant coupling levels are no longer horizontal. A reference line corresponding to -34 db below direct coupling is shown on top in Fig. 2-5. This reference level was obtained by connecting directly between flanges A and B (Fig. 2-1) while introducing 34 db attenuation by means of the precision attenuator. This attenuation was then removed from the system during the actual coupling measurement.

Patterns of coupling versus receiver orientation were also taken but are not presented since they do not contain any new information beyond that previously published data (Lyon, Kalafus, et al, 1966), except of course for the overall coupling level.

2.2.2 Slots

A slot was recessed in a shallow cavity which was partially filled with absorber. The cavity dimensions and absorber geometry and type are the same as the ones used with the E-Sectoral Horn (Fig. 2-2). This modification was found to increase the maximum gain of the slot by approximately 0.5 to 1.0 db throughout the X-band while decreasing the radiation along the surface of the ground plane. Typical radiation patterns taken at a frequency of 10 GHz are presented in Fig. 2-6.

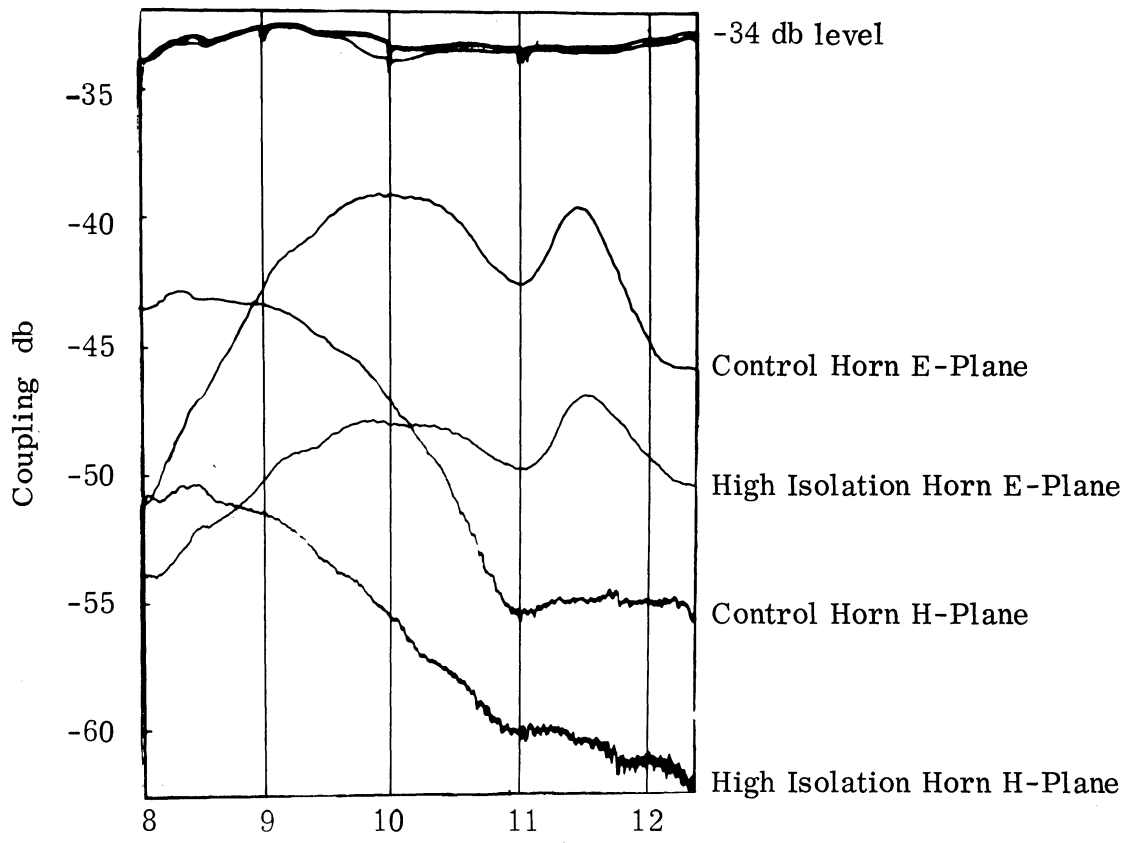

FIG. 2-5: E- AND H-PLANE COUPLING VERSUS FREQUENCY FOR TWO E-SECTORAL HORNS SPACED 11.43 cm. (Eccosorb MF-124 Absorber).

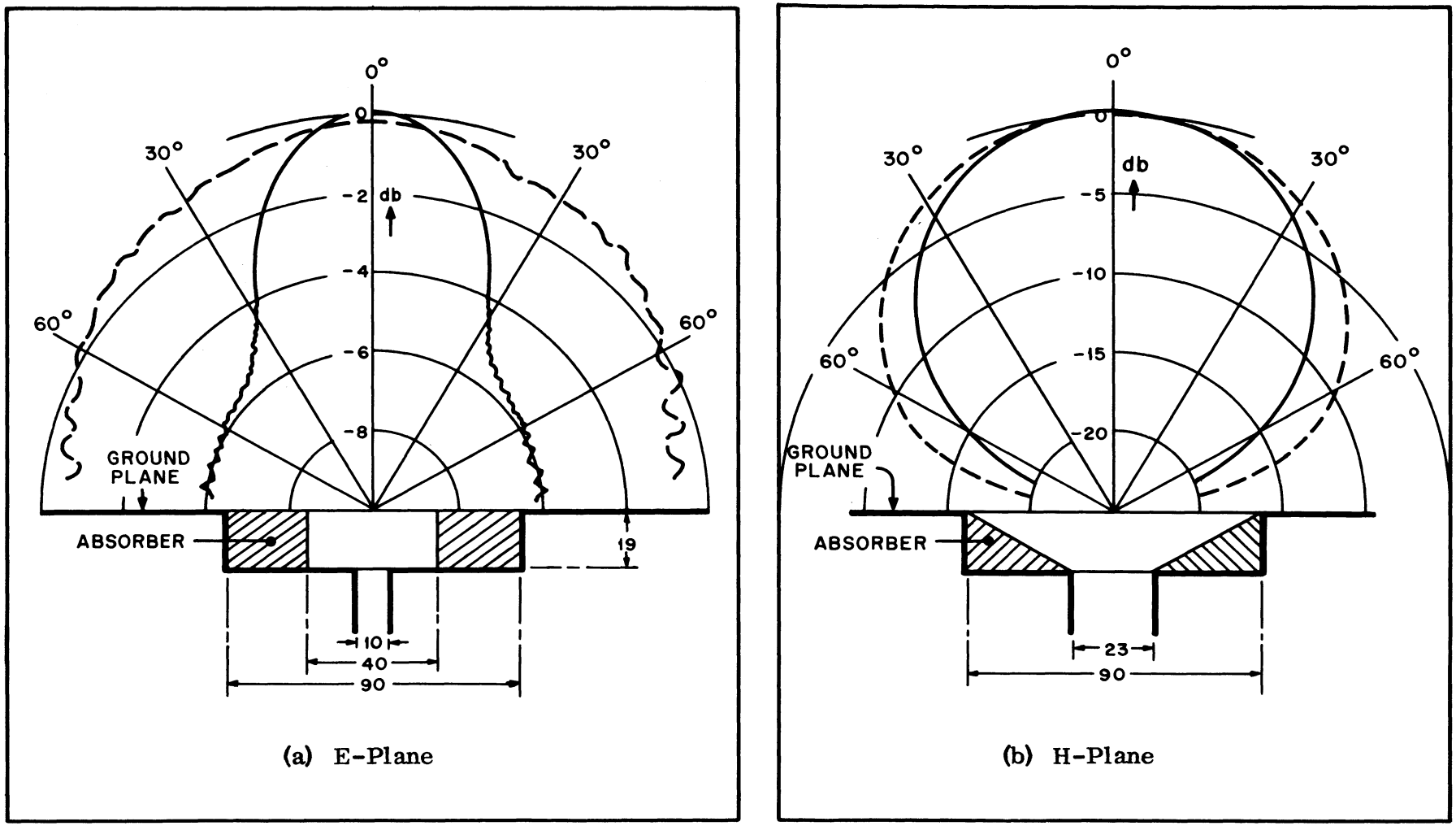

FIG. 2-6: SLOT IN CAVITY WITH ABSORBER (Eccosorb MF-124) ANTENNA GEOMETRY AND FAR-FIELD RADIATION PATTERNS AT 10 GHz (Dashed Lines Show Corresponding Radiation Patterns of Plain Slot Dimensions in cm).

The E-plane coupling between a modified and a plain slot is shown in Fig. 2-7, where it is also compared to the coupling between two plain slots. A reduction of maximum coupling by 6.5 db is observed over the X-band of frequencies. Again, by reciprocity, if both antennas were similarly modified, a 13 db decoupling would result.

Next the absorber was changed to B.F. Goodrich's RF-X (same geometry). Variation of maximum gain and coupling with frequency as well as radiation patterns for this case are shown in Figs. 2-8 through 2-10. It should be noted that very similar patterns to those shown in Figs. 2-8 to 2-10 were observed when no absorber at all was placed in the cavity, indicating that the RF-X absorber is not suitable for this application.

2.3 Decoupling of Two Antennas by Means of Chokes and Corrugations

2.3.1 Chokes

A new slot antenna was constructed having an X-band slot surrounded by four chokes in the form of circumferential trenches. If b is the radius of such a choke then the cutoff depth is given by

$$d_c = \frac{\lambda_g}{4} = \frac{\lambda_o}{4\sqrt{1 - \left(\frac{\lambda_o}{2\pi b}\right)^2}} \qquad (\lambda_o = \text{free space wavelength}) \ .$$

Since previous data (Lyon, et al, 1966) have indicated that for frequencies below the cutoff the gain of the antenna is decreased, while the coupling to nearby antennas is increased, the chokes were designed with a cutoff frequency of 8.2 GHz, The antenna gain was found to increase by 4 db at this frequency (Fig. 2-11) due to the deformation of the radiation pattern of the slot caused by the chokes (Fig. 2-12).

The E-plane coupling between a slot surrounded by four chokes and a plain slot was 11.5 db below the coupling between two plain slots at the cutoff frequency

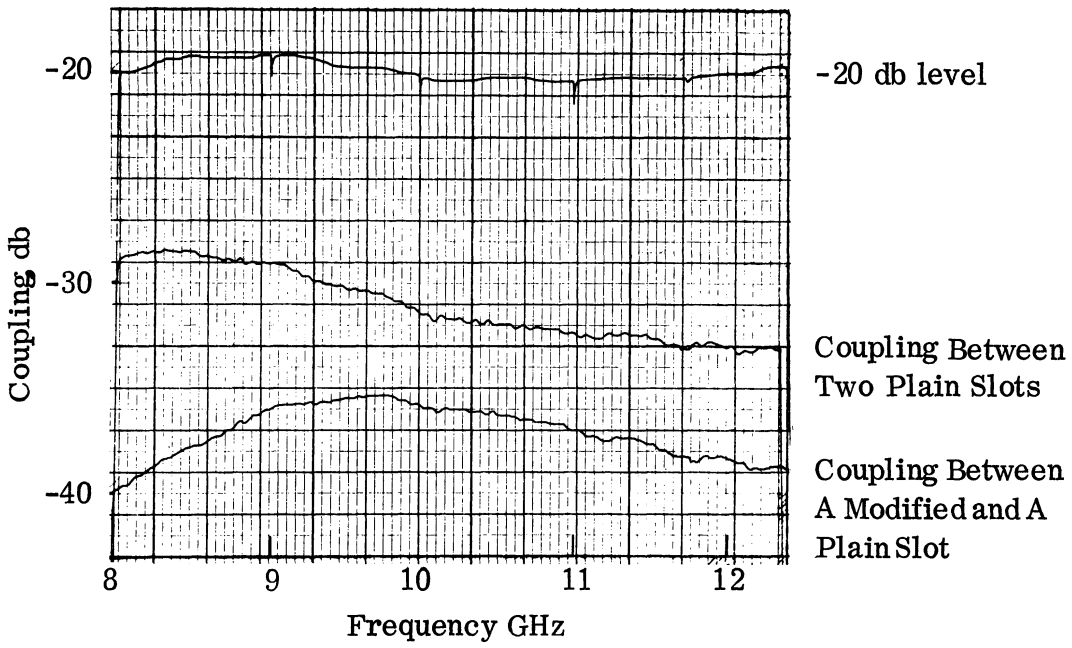

FIG. 2-7: E-PLANE COUPLING VERSUS FREQUENCY FOR TWO SLOTS SPACED 11.43 cm (Absorber Eccosorb MF-124).

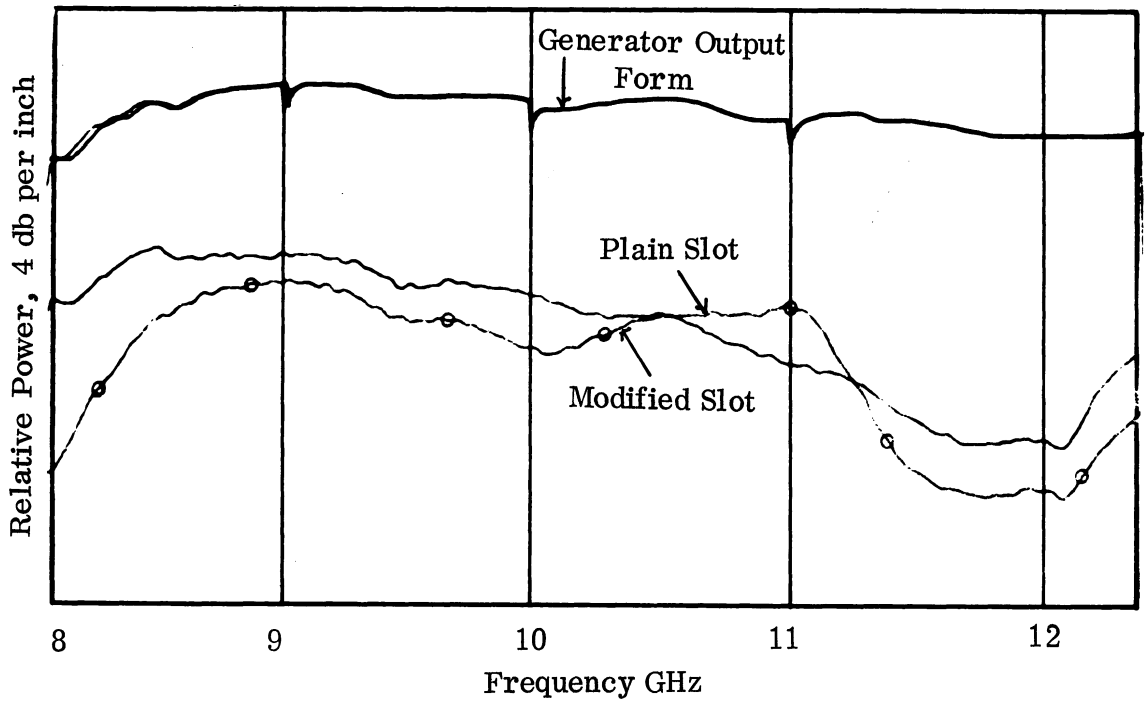

FIG. 2-8: MAXIMUM GAIN VERSUS FREQUENCY FOR SLOTS (Absorber: B.F. Goodrich RF-X).

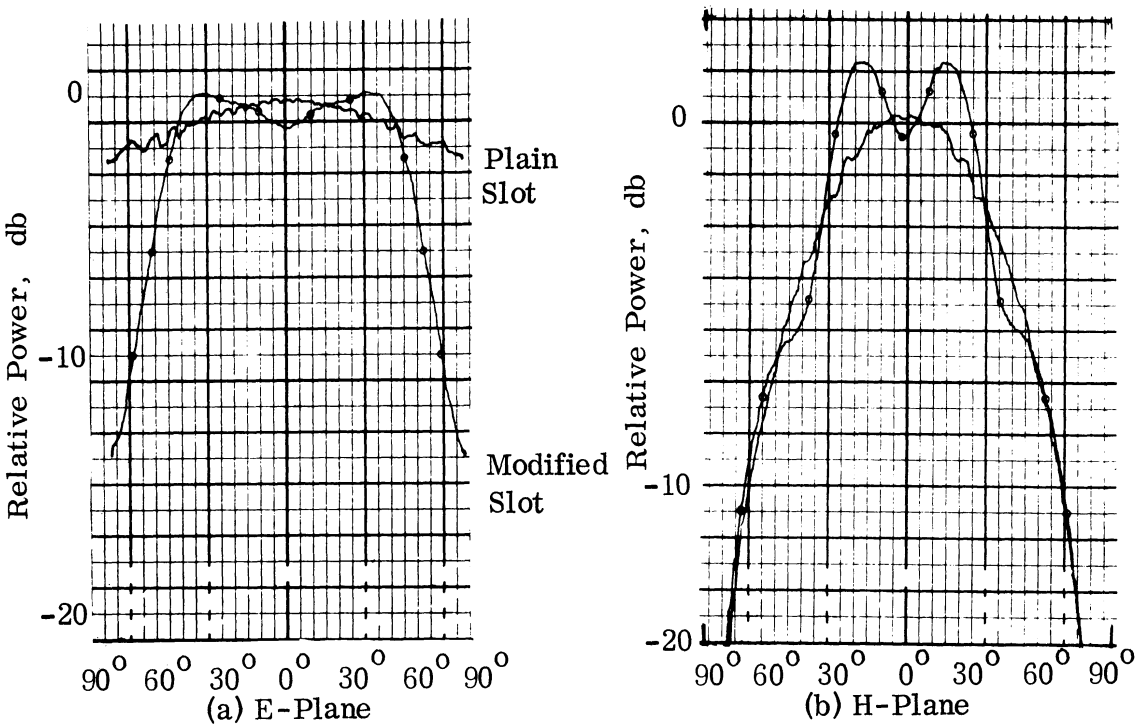

FIG. 2-9: E- AND H-PLANE RADIATION PATTERNS AT 10 GHz.

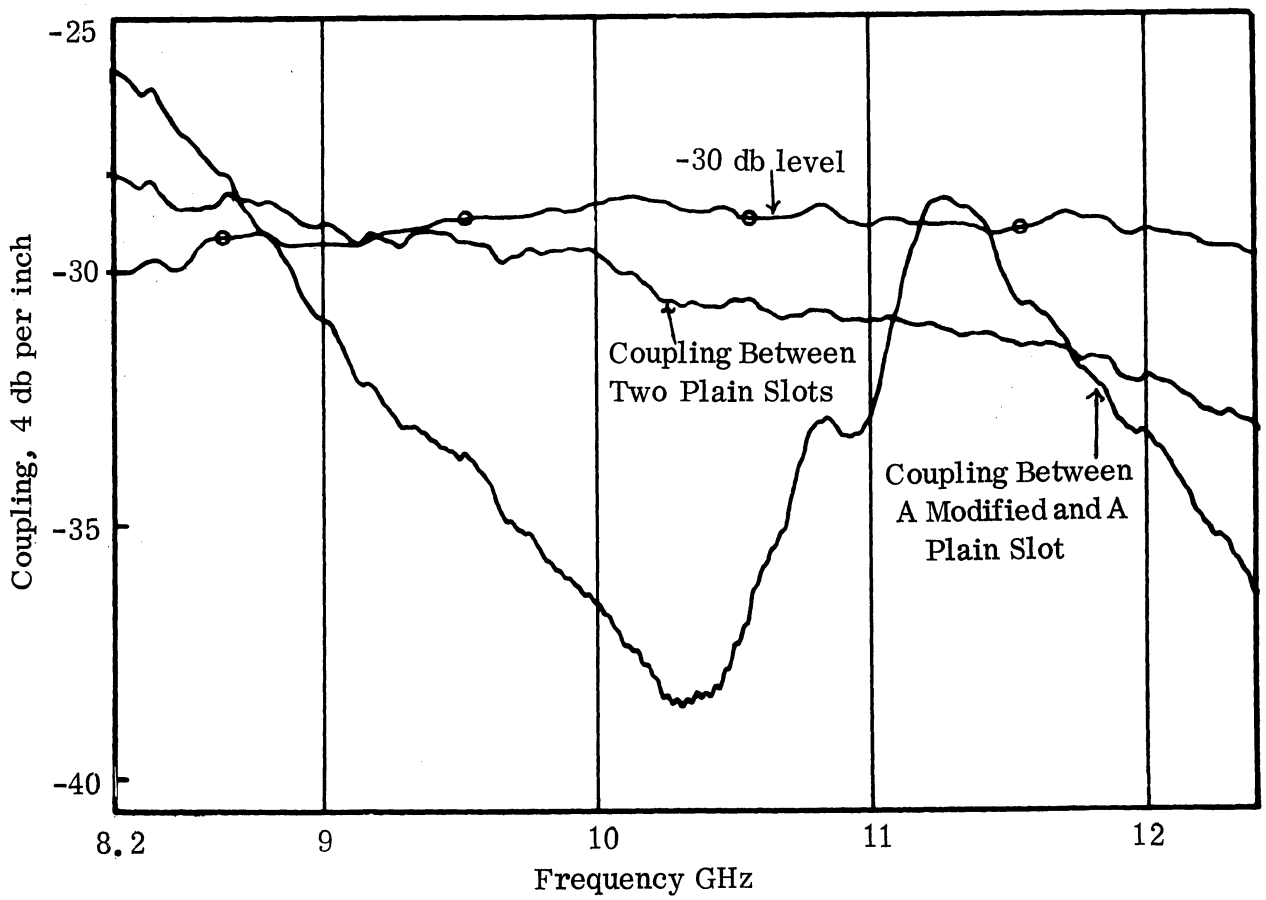

FIG. 2-10: E-PLANE COUPLING VERSUS FREQUENCY FOR TWO SLOTS SPACED 11.43 cm. (Absorber: B.F. Goodrich RF-X).

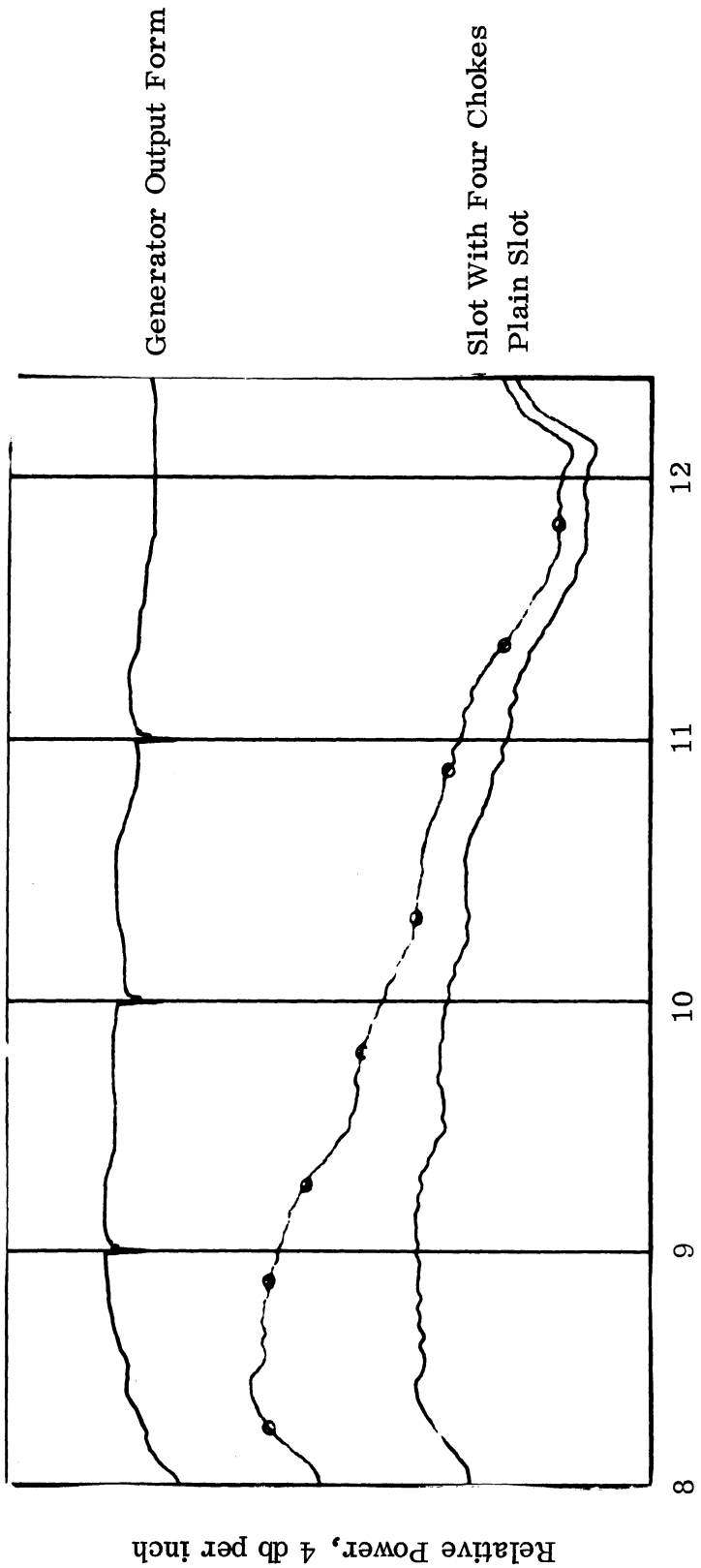

FIG. 2-11: MAXIMUM GAIN VERSUS FREQUENCY FOR SLOTS.

(Fig. 2-13). This decoupling, however, was gradually reduced at the higher frequencies. Thus the decoupling over the entire X-band, would be approximately 13 db if both slots were surrounded by chokes. The H-plane coupling was very little affected by the presence of chokes. The decoupling observed was of the order of 1 to 2 db.

2.3.2 Corrugations

The propagation of an electromagnetic wave along an infinite corrugated surface has been studied (Hurd, 1954). The data in this reference show that the cutoff depth, d_c, depends upon the spacing of the corrugations, t. For a separation $t \leq \frac{\lambda_o}{10}$, then $d_c = 0.23\lambda_o$ to $0.25\lambda_o$. The surface wave does not propagate for $d_c < d < \frac{\lambda_o}{10}$.

Three sets of corrugations have been used during this period. All three were imbedded in a cavity placed symmetrically between two slots, oriented for E-plane coupling. The aperture dimensions of this cavity were 7.2 cm and 2.3 cm parallel to the H- and E-plane respectively. The depth of the cavity was adjustable so that the corrugations would be always flush-mounted. The parameters of the sets of corrugations used are given below:

Set I: $d_1 = 0.9$ cm $t_1 = 1.5$ mm

Set II: $d_2 = 0.9$ cm $t_2 = 2.1$ mm

Set III: $d_3 = 0.6$ to 0.9 cm $t_3 = 1.5$ mm .

In the third set the depth was varied in equal steps monotonically, so that in an E-plane cross-section the bottom of the cavity would be in a ladder form.

The sets I and II had almost identical radiation patterns (within 0.2 db) which seemed to be greatly influenced by the existence of the cavity as shown in Fig. 2-14a. Set III created a radiation pattern of the same general shape but with

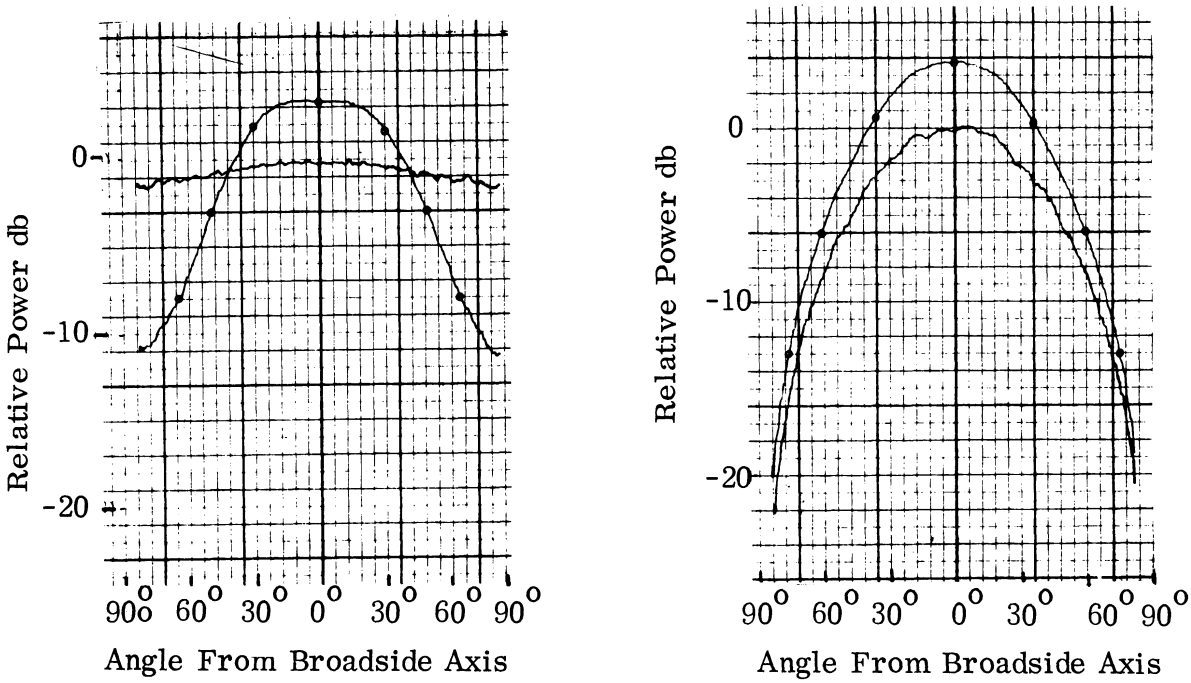

FIG. 2-12: E- AND H-PLANE RADIATION PATTERNS AT 8.23 GHz, (——) Plane Slot ; (—o—) Slot With Four Chokes.

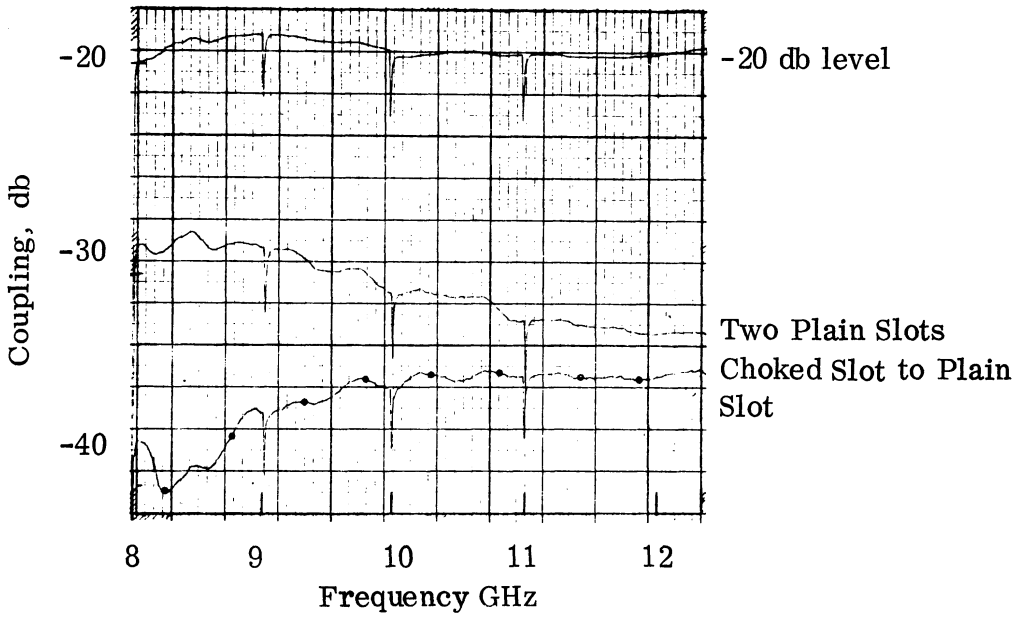

FIG. 2-13: E-PLANE COUPLING VERSUS FREQUENCY FOR TWO SLOTS SPACED 11.43 cm.

different size side lobes (Fig. 2-14b). The maximum gain in the presence of the tapered corrugations was +1 to -2 db with respect to the gain of the plain slot, depending upon the frequency.

The decoupling obtained was of the order to 5 to 8 db (Fig. 2-15). In view of the decoupling levels observed and the accompanying reduction of gain at the broadside direction, this method at its present stage of development is not considered satisfactory for coupling reduction. It should be noted, however, that the tapered corrugations offer more decoupling without any additional loss in gain. The design of improved tapered corrugations with desirable a frequency characteristic will be attempted in the future.

2.4 Decoupling of Two Antennas by Means of Parasitic Elements

Parasitic elements can be used as reflectors or directors to reflect or direct, respectively, the antenna radiation in a particular direction. Such elements have been found to be very effective at VHF and UHF frequencies (e.g., Yagi-Uda Array) and have numerous applications.

The use of parasitic elements with microwave aerospace antennas is severely restricted by the requirement of flush-mounting. In initial experiments good results were obtained by using four screws errected on the ground plane between two E-Sectoral Horns. In this case the E-plane coupling was reduced by 18 db over a frequency range of 0.5 GHz (9.25 to 9.75 GHz).

In order to study the behavior of flush-mounted parasitic antennas a new antenna has been constructed in the form of a three slot array. One slot was fed by X-band waveguide while the other two were backed by cavities constructed again from X-band waveguide and equipped with sliding shorts. The distance of the parasitic slots from the transmitting one was adjustable, from a minimum of 1.27 cm center-to-center (imposed by the physical dimensions of the waveguide) to a maximum of approximately 4.0 cm.

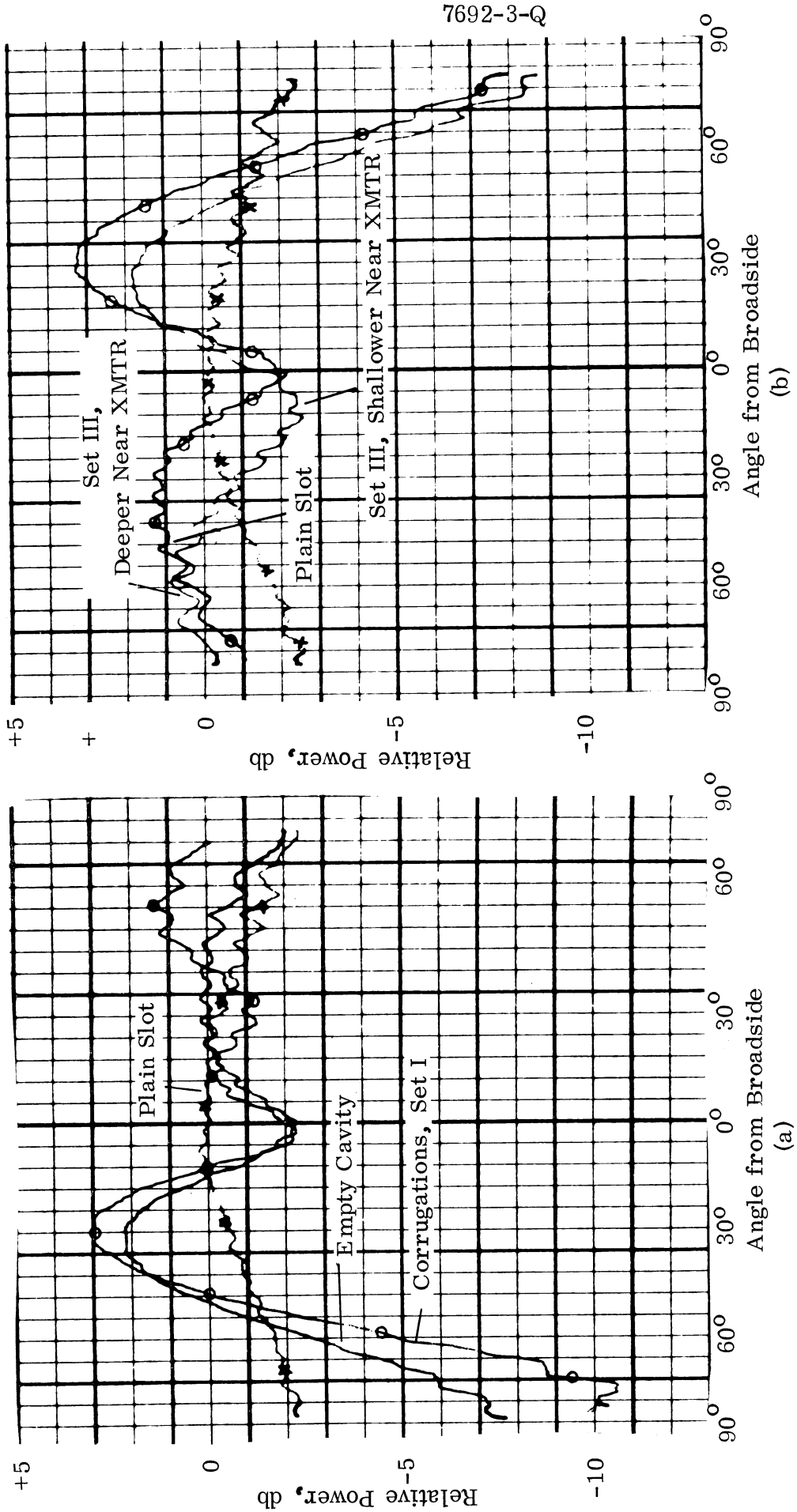

FIG. 2-14: E-PLANE RADIATION PATTERNS OF SLOT IN THE PRESENCE OF CAVITY AND CORRUGATIONS AT 10 GHz.

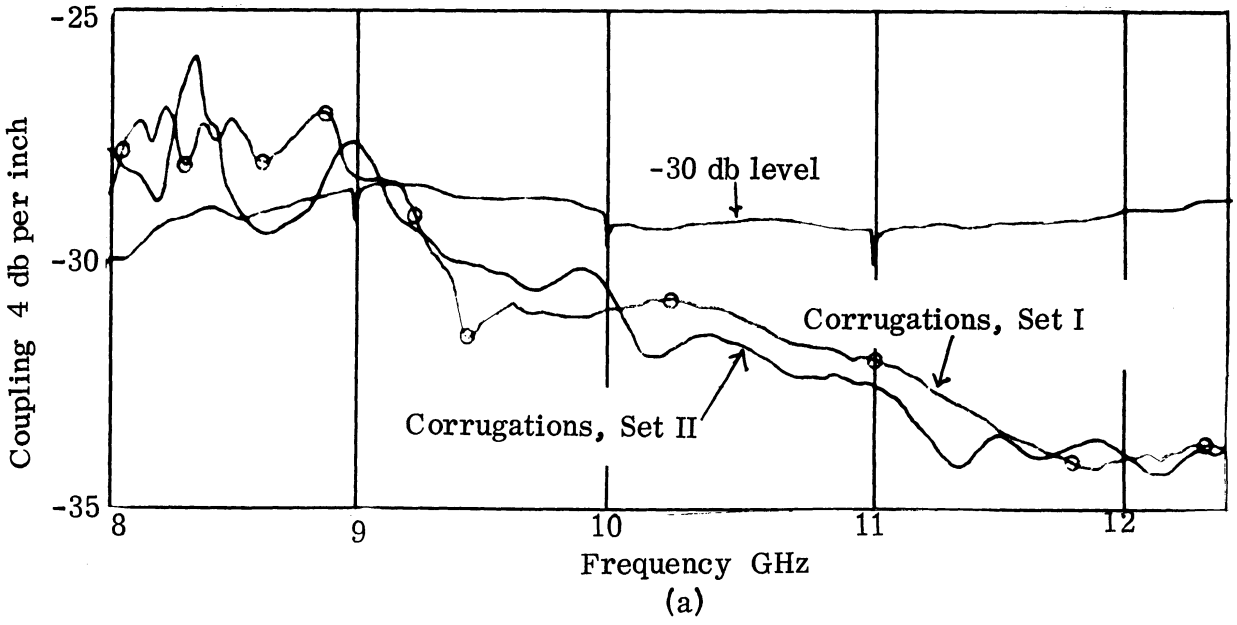

(a)

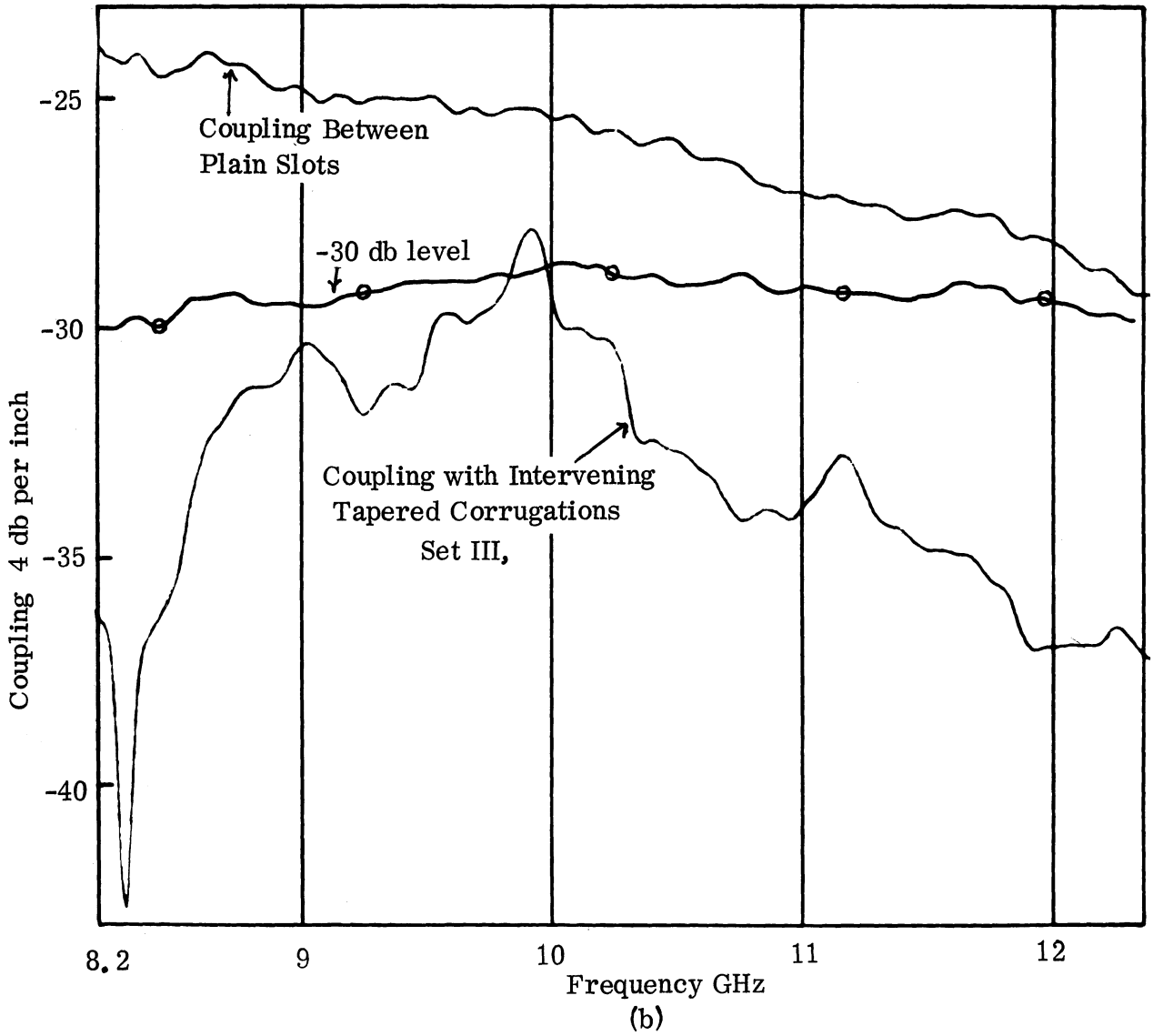

(b)

FIG. 2-15: COUPLING VERSUS FREQUENCY FOR TWO SLOTS SPACED 6.5 cm WITH AND WITHOUT INTERVENING CORRUGATIONS.

The case does not lend itself readily for an exact theoretical analysis because the close spacing of the parasitic elements necessitates solution of the combined problem, transmission line - - antenna, i.e., one would have to consider the field distribution in the aperture of the transmitting slot as unknown. If one were to use "thin" slots then the field distribution in the transmitting slot may be assumed known and on this basis the problem can be solved, with the aid of a digital computer (Coe, et al, 1964).

A series of radiation patterns have been taken for various spacings, ℓ, of the parasitic elements and various positions of the shorting plungers. A single parasitic element acts as a reflector when the cavity depth d is $\lambda_g/4$. A front to back ratio of 7 db was observed for close spacings. For the minimum possible spacing the pattern becomes highly asymmetrical while for spacings near $\lambda_g/2$ (center-to-center) the pattern symmetry is partially restored (Fig. 2-16). No setting was found for which a single parasitic element would act as "director", increasing the side lobe level in its direction. In combinations of two parasitic elements on either side of the transmitter it was noted that the "reflecting" parasitic had a predominant effect. A front-to-back ratio of 8 db has been obtained in this case (Fig. 2-17).

Coupling measurements have not been completed yet. So far a modest decoupling of 3 db has been observed if one of the two slots of a transmitter-receiver system is accompanied by parasitic elements. Twice as much would be expected if both slots were similarly modified. It is felt that considerable improvement will be possible in the near future.

2.5 Decoupling of Two Antennas by Means of an RF Bridge

If two antennas are in proximity to each other, there may be strong interference or "coupling" between them. An RF bridge has been used to reduce this interference, or to "decouple" the two antennas.

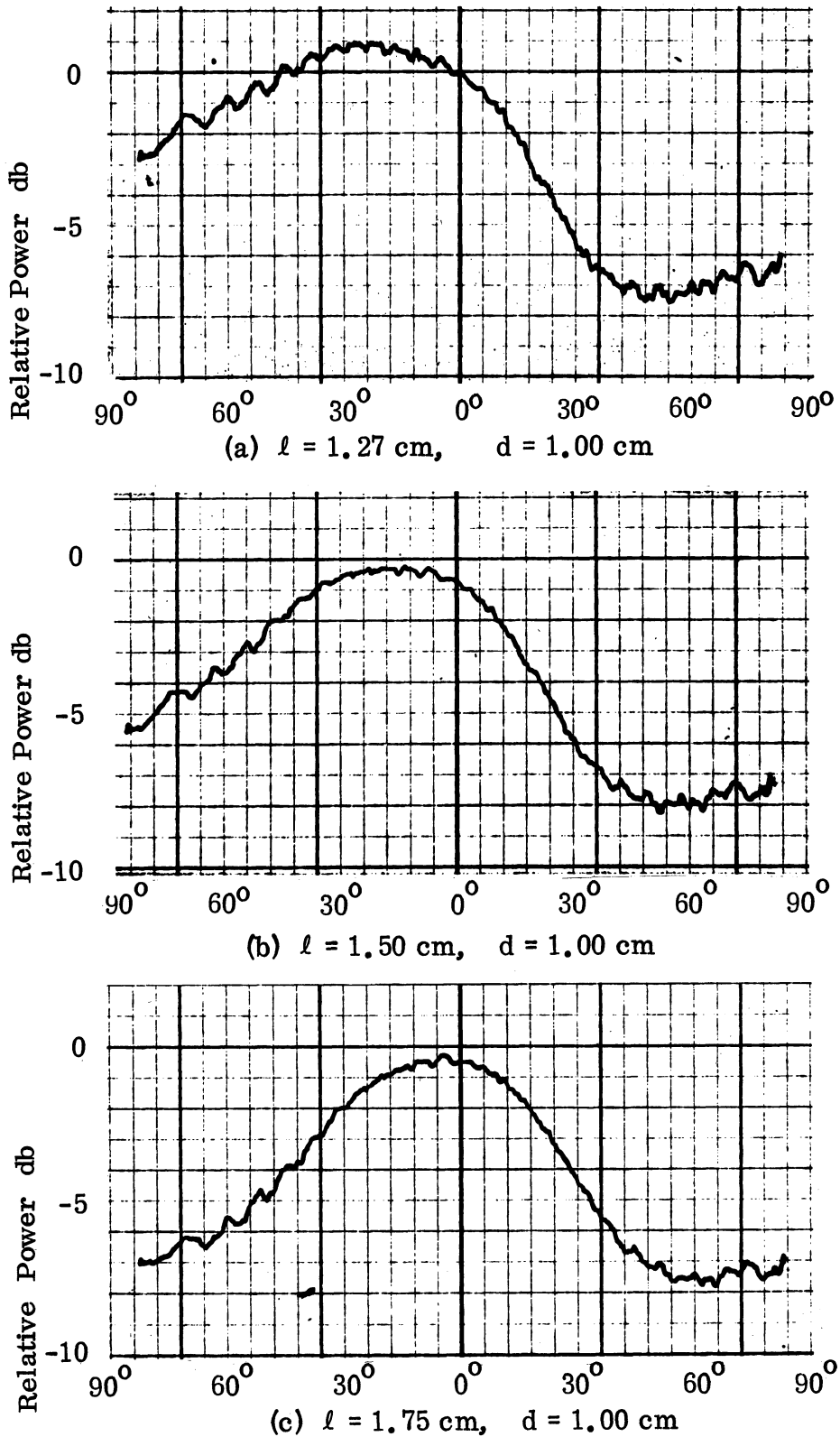

FIG. 2-16: E-PLANE RADIATION PATTERNS OF A SLOT IN THE PRESENCE OF ONE PARASITIC SLOT, ON THE RIGHT, AT 10 GHz. (ℓ = center-to-center spacing).

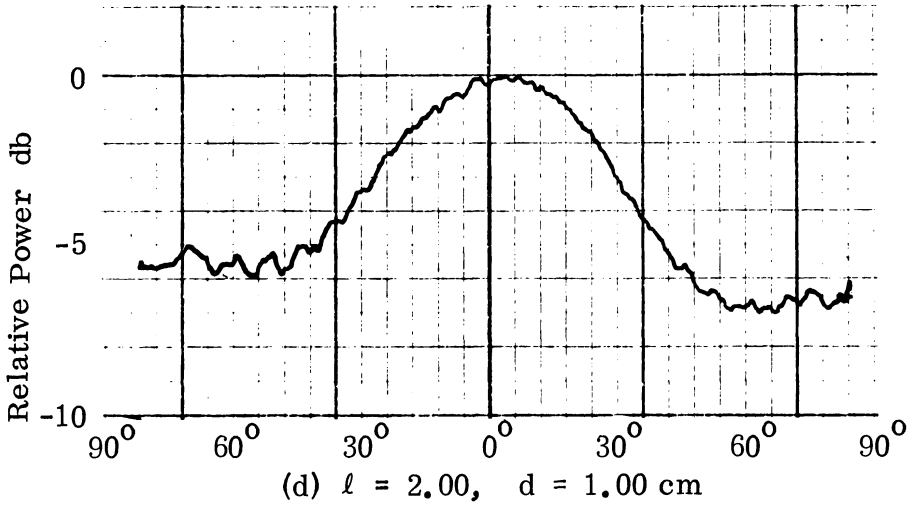

(d) ℓ = 2.00, d = 1.00 cm

FIG. 2-16: E-PLANE RADIATION PATTERNS OF A SLOT IN THE PRESENCE OF ONE PARASITIC SLOT, ON THE RIGHT, AT 10 GHz. (ℓ = center-to-center spacing).

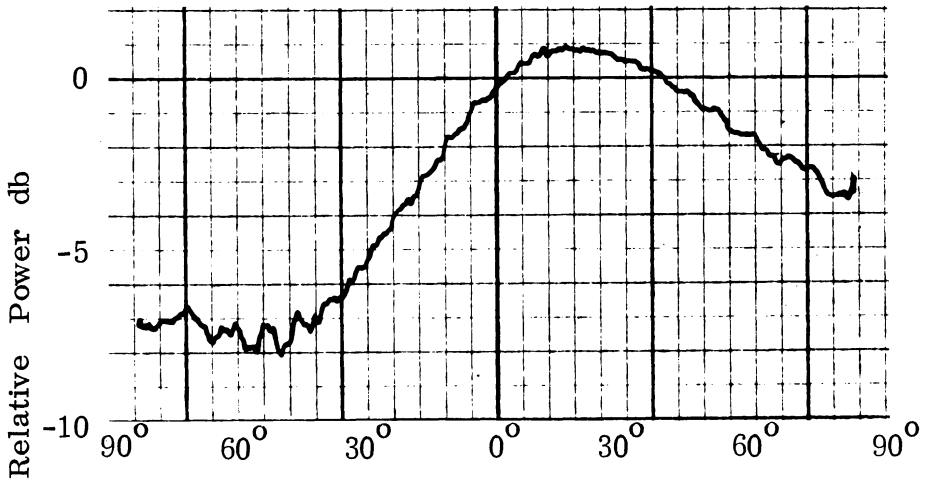

Parasitic 1 Transmitter Parasitic 2

ℓ_1 = 1.27 cm ℓ_2 = 1.27 cm

d_1 = 0.99 cm d_2 = 1.98 cm

FIG. 2-17: E-PLANE RADIATION PATTERN OF A SLOT IN THE PRESENCE OF TWO PARASITIC SLOTS AT 10 GHz

The basic concept of the RF bridge is illustrated in Fig. 2-18. The interfering signal travels from the transmitter to the receiver along the upper path of length d_1 cm (equivalent air path length). This signal path is called the coupled path. The RF bridge cancels out this interfering signal by producing a signal at the receiver which is of the same amplitude as the interfering signal, but 180^o out of phase with it. This canceling signal travels from the transmitter to the receiver along the lower path of length d_2 cm (equivalent air path length). This signal path is called the bridge path and contains an adjustable phase shifter, labelled ϕ in the figure.

Consider first the coupled path. The number of waves which can be contained in a distance x is given by:

$$N = x/\lambda \tag{2.1}$$

where λ is the wavelength. The wavelength function is determined by the medium through which the wave propagates. As a simplification distances d are expressed as equivalent air path lengths in cms. For free space:

$$\lambda_o = c/f = \frac{3 \times 10^{10} \text{ (cm/sec)}}{f \text{ (Hertz)}} \quad . \tag{2.2}$$

Now, if the transmitter is taken as the phase reference in Fig. 2-18, the wave arrives at the receiver along the coupled path with the phase:

$$\theta_1 = (d_1/\lambda_o - n_1) \times 360^o \quad . \tag{2.3}$$

Where d_1/λ_o is the number of waves along the coupled path, and n_1 is the greatest integer $\leq d_1/\lambda_o$. The subtraction of n_1 in Eq. (2.3) is done so $0^o \leq \theta_1 \leq 360^o$. See Fig. 2-19 for a wave arriving at the receiver with phase

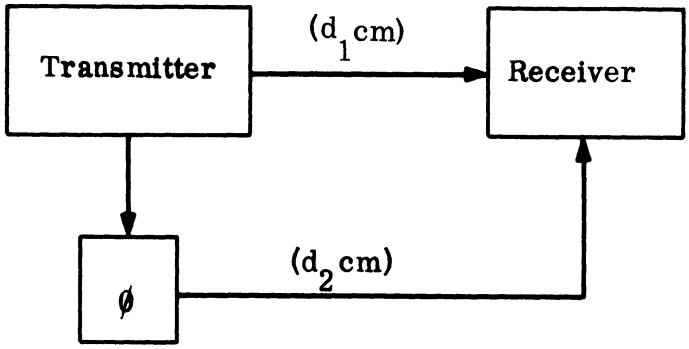

FIG. 2-18: BASIC R.F. BRIDGE

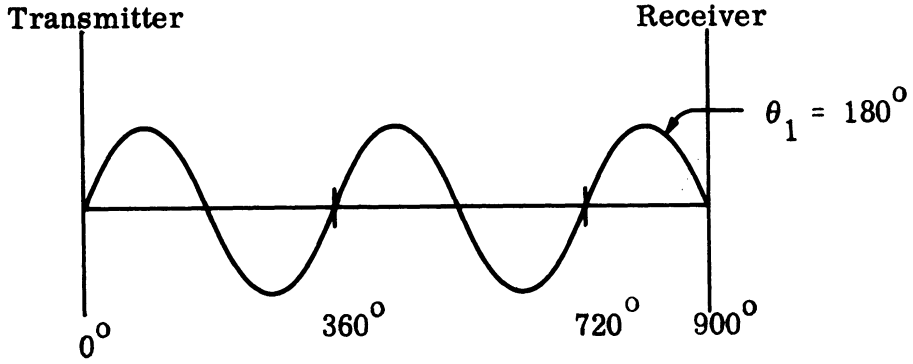

FIG. 2-19: WAVE ARRIVING AT RECEIVER WITH PHASE $\theta_1 = 180^o$

$\theta_1 = 180^o$ along the coupled path. In the figure, $d_1/\lambda_o = 2.5$ waves.

Now consider the bridge path. It is similar to the coupled path except that it contains a phase-shifter which adds ϕ^o to the phase angle in this path. ($0^o \leq \phi^o \leq 360^o$) Again, taking the transmitter as the phase reference, the wave arrives at the receiver along the bridge path with the phase:

$$\theta_2 = (d_2/\lambda_o - n_2) \times 360^o + \phi^o \quad . \tag{2.4}$$

For the RF bridge to produce decoupling, the signal along the bridge path must cancel the signal from the coupled path. Thus, at the receiver:

$$\left| \theta_1 - \theta_2 \right| = 180^o \quad . \tag{2.5}$$

Combining Eqs. (2.3) and (2.4) yields:

$$\left| \frac{1}{\lambda_o} (d_1 - d_2) 360^o - \phi^o \right| - n(360^o) = 180^o \tag{2.6}$$

where n is an integer.

Obtaining broadband decoupling with the RF bridge is very important. The manner in which the decoupling varies with frequency must be known. Equation (2.6) provides much insight into this problem.

In a physical example, the lengths of the coupled path and the bridge path will be fixed at d_1 cm and at d_2 cm respectively. The phase-shifter will be set at a phase angle of ϕ_1^o to cancel the interfering signal at a frequency of f_1 Hertz, corresponding to a wavelength of λ_1 cm.

Because Eq. (2.6) deals with degrees, it is periodic with cycles of 360^o. Thus, the bridge will null at a wavelength of λ_i, corresponding to f_i, when:

$$1/\lambda_1 - 1/\lambda_i = K \; 1/(d_1 - d_2) \qquad (2.7)$$

where K takes on values of positive integers.

Then, for a single setting of ϕ, the bridge will cancel the interfering signal at many frequencies. This happens whenever a frequency corresponds to an integral number of wavelengths, as shown in Eq. (2.7). However, just as the bridge will null at many frequencies, there are also many frequencies where the bridge path's signal will add in-phase with the coupled signal at the receiver. This adding will actually increase the level of the interfering signal at those frequencies. This is undesirable.

The difference in length between d_1 and d_2 is the key to making the RF bridge feasible. If d_1 equals d_2, the coefficient of the frequency dependent term in Eq. (2.6) will be zero. For this case, $\phi = 180^\circ$ is a requirement to null the bridge, independent of frequency. The decoupling obtained would be perfectly broadband. Moreover, there would be no in-phase adding of signals as described earlier.

Figure 2-20 shows the relationship of d_1 to d_2. When d_1 equals d_2, the decoupling is broadband as discussed above. When the difference between d_1 and d_2 is moderate, the nulls are fairly broad and moderately spaced in frequency. When the difference between d_1 and d_2 is large, the nulls are very narrow and closely spaced. Note the in-phase adding that actually increases the coupling which occurs whenever d_1 is not equal to d_2.

Thus, for the postulated RF bridge in Fig. 2-18, the decoupling obtained could be perfectly broadband if d_1 equals d_2.

2.5.1 A Microwave Bridge to Decouple Two Slot Antennas (X-Band)

The circuit of a microwave bridge used to decouple two slot antennas mounted on a common ground plane is shown in Fig. 2-21. This bridge circuit is designed

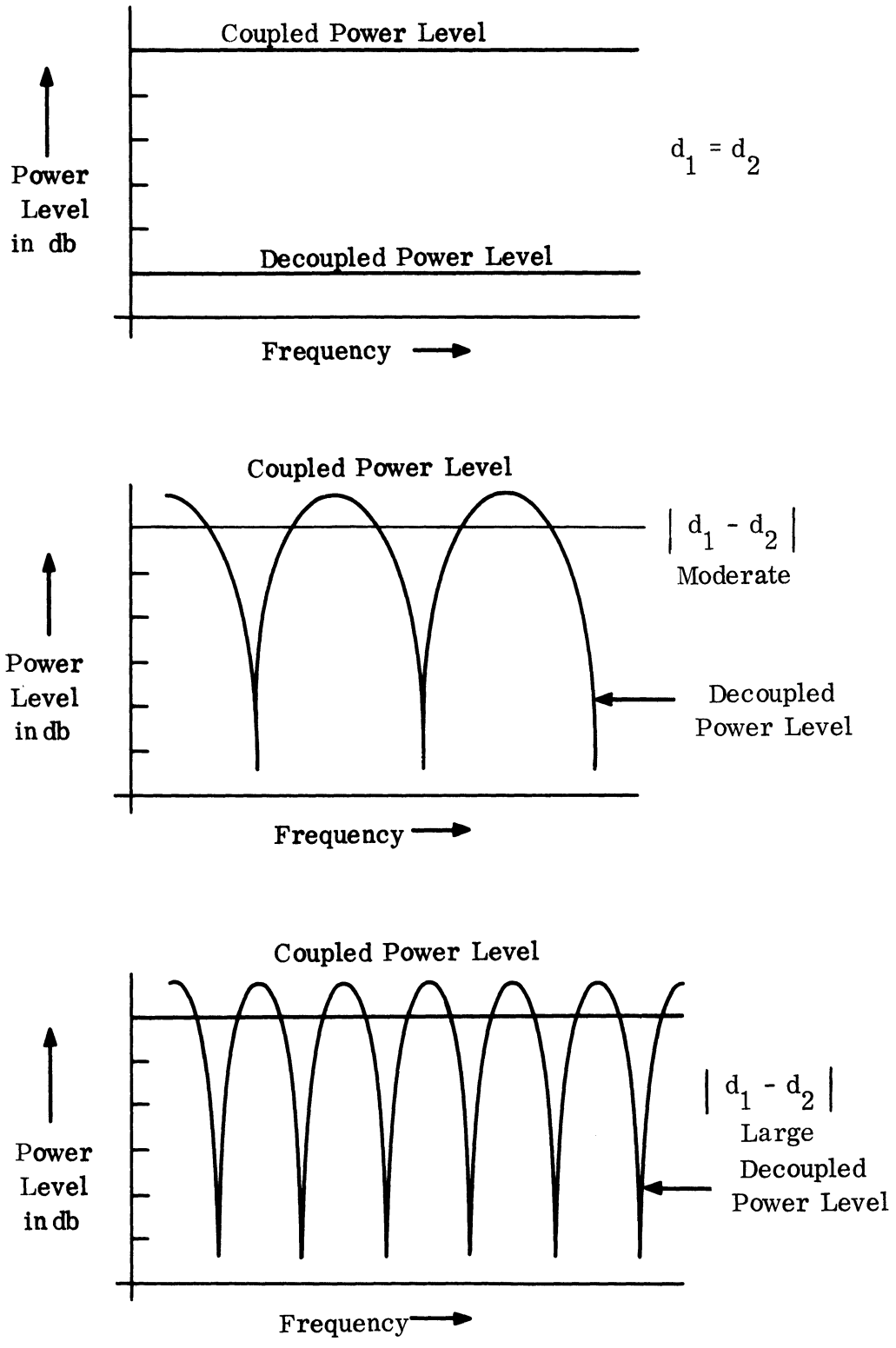

FIG. 2-20: EFFECT OF $|d_1 - d_2|$ ON DECOUPLING.

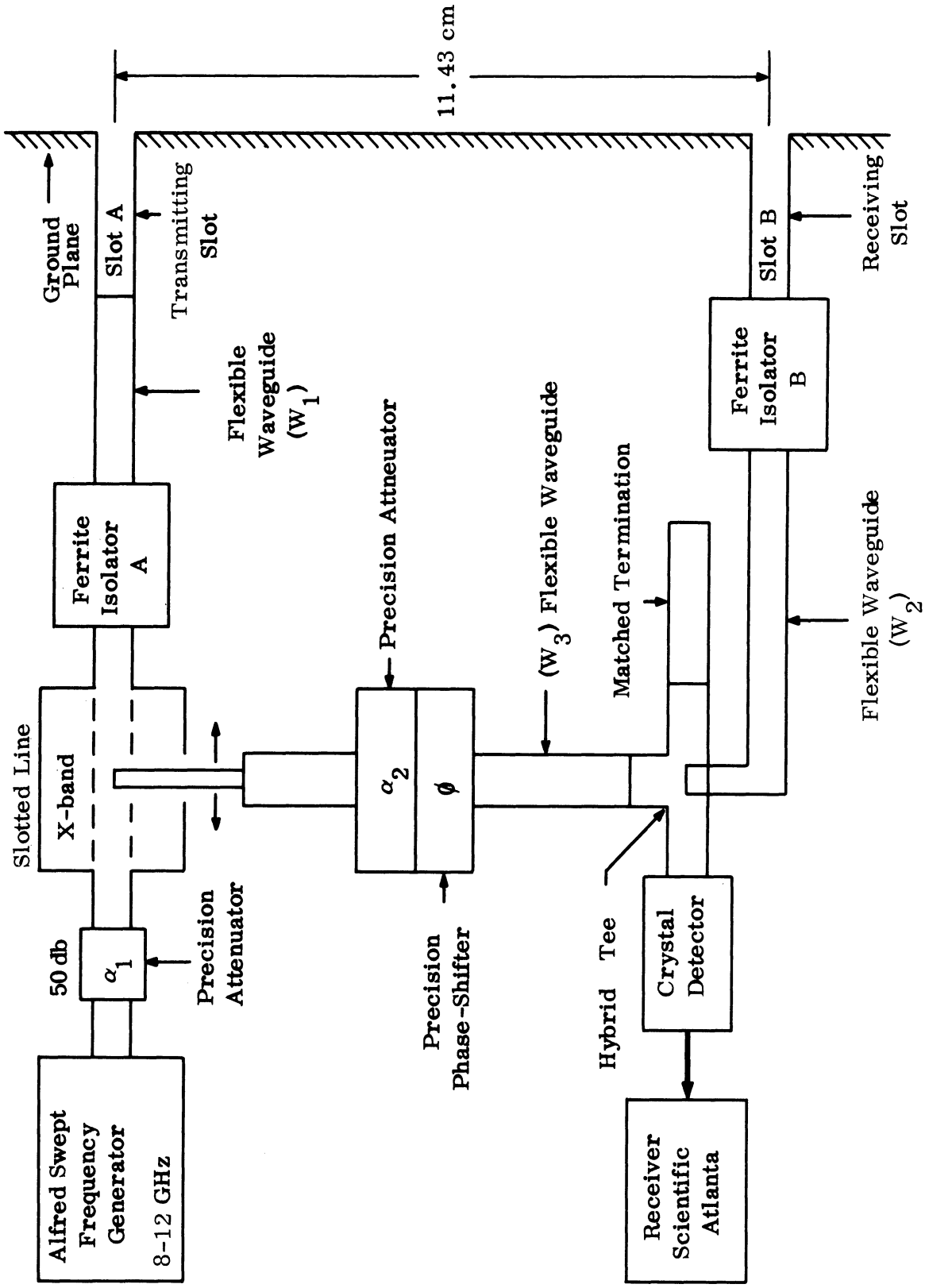

FIG. 2-21: MICROWAVE BRIDGE

for X-band and has been built entirely with X-band waveguide components. RF power is supplied by an Alfred X-band swept-frequency generator. The input power level is adjusted by the precision attenuator α_1.

It has been shown that broadband decoupling is possible with an RF bridge if the length of the coupled path is made equal to the length of the bridge path. The reference point which was the transmitter in Fig. 2-18 is the probe of the X-band slotted line in Fig. 2-21. The coupled path begins at the probe, includes the rest of the slotted line, the ferrite isolator A, the flexible waveguide section W_1, the transmitting antenna slot A, the coupling path between slot A and slot B, the receiving antenna slot B, the ferrite isolator B, and the flexible waveguide section W_2. The bridge path also begins at the probe of the slotted line. It includes the probe, the attenuator α_2, the phase-shifter ϕ, and the section of flexible waveguide W_3. The bridge signal and the coupled signal are added together in the hybrid tee. The resultant output passes through a crystal detector into the Scientific Atlanta receiver. The bridge path and the coupled path are made approximately equal in length by a careful choice of the lengths of the flexible waveguide sections. A fine adjustment of the coupled path length is provided by the slotted line. The probe rides in a movable carriage; the range of adjustment is 10 cm.

The probe in the slotted line provides the signal for the bridge path. The precision attenuator α_2 matches the level of the bridge signal to the level of the coupled signal. For the separation of the two slots shown, the loss of signal power is approximately 30 db between the transmitting slot and the receiving slot. The precision phase-shifter provides the necessary phase shift for the bridge signal to cancel the coupled signal at the hybrid tee. The ferrite isolators are used to prevent standing waves which might be caused by mismatches between the various components.

An analysis of the microwave bridge circuit can be performed like the analysis of the general RF bridge. The expression for the arriving phase angle in the bridge path is basically the same as the earlier expression for θ_2 (Eq (2.4)). For waveguide, however, the relationship between the wavelength and the frequency is known:

$$\lambda_g = c/f \times 1/\sqrt{1 - (c/f\,\lambda_c)^2} \qquad (2.8)$$

where λ_c is the cutoff wavelength = 4.57 cm for X-band waveguide. Then, substituting this λ_g into Eq. (2.4):

$$\theta_2 = (d_2/c \times f\sqrt{1 - (c/f\,\lambda_c)^2} - n_2)\,360^\circ + \phi^\circ \qquad (2.9)$$

where d_2 is the length of the waveguide in the bridge path.

In the coupled path, however, the wave travels through two different media. There is X-band waveguide, and there is the air path between slot A and slot B. Thus, there are two terms in the equation for the arriving phase angle:

$$\theta_1 = (dwg/\lambda_g + dair/\lambda_o - n_1) \times 360^\circ \qquad (2.10)1$$

where dwg is the length of waveguide in the coupled path and dair is the length of the air path between Slot A and slot B. Substituting the expressions for λ_g (Eq. (2.8)) and λ_o (Eq. (2.2)) into Eq. (2.10) we get:

$$\theta_1 = ((dwg/c) \times f\sqrt{1 - (c/f\,\lambda_c)^2} + (dair/c) \times f - n_1)\,360^\circ. \qquad (2.11)$$

Next, define a factor S, a function of frequency alone:

$$S = f/c \times \sqrt{1 - (c/f\,\lambda_c)^2} \times 360^o \quad . \tag{2.12}$$

As before, if the microwave bridge is to work, θ_1 and θ_2 must be 180^o apart. Expressed in an equation using the factor S:

$$\left| S\,(dwg - d_2 + dair/\sqrt{1 - (c/f\,\lambda_c)^2}) - \phi^o \right| - n\,360^o = 180^o \tag{2.13}$$

Equation (2.13) is similar to the RF bridge Eq. (2.6). The factor S, which is a function of frequency only, is similar to $(360^o/\lambda)$ in Eq. (2.6). Before, we set d_1 equal to d_2 and the coefficient of the frequency dependent term went to zero. We want to do the same thing in Eq. (2.13). But looking above, we see that the coefficient of S has a part that is frequency dependent itself. Thus, the coefficient of S cannot be made to go to zero for all frequencies. Thus, we see that the microwave bridge of Fig. 2-21 does not produce perfectly broadband decoupling. However, the best performance would be obtained when the coefficient of S is as small as possible.

Using the microwave bridge of Fig. 2-21, we have been able to obtain about 15 db of decoupling over a bandwidth of 1.5 GHz in the X-band. The frequency where the decoupling occurs is variable in this band. Figures 2-22 through 2-25 illustrate the decoupling obtained with the microwave bridge in X-band. Figure 2-26 is included to show what happens if the coefficient of S in Eq. (2.13) is too large.

2.5.2 Proposed Improvements of the X-Band Microwave Bridge

In the precious section, the reason the decoupling was not more broadband is mainly the presence of the air coupling path between slot A and slot B. This

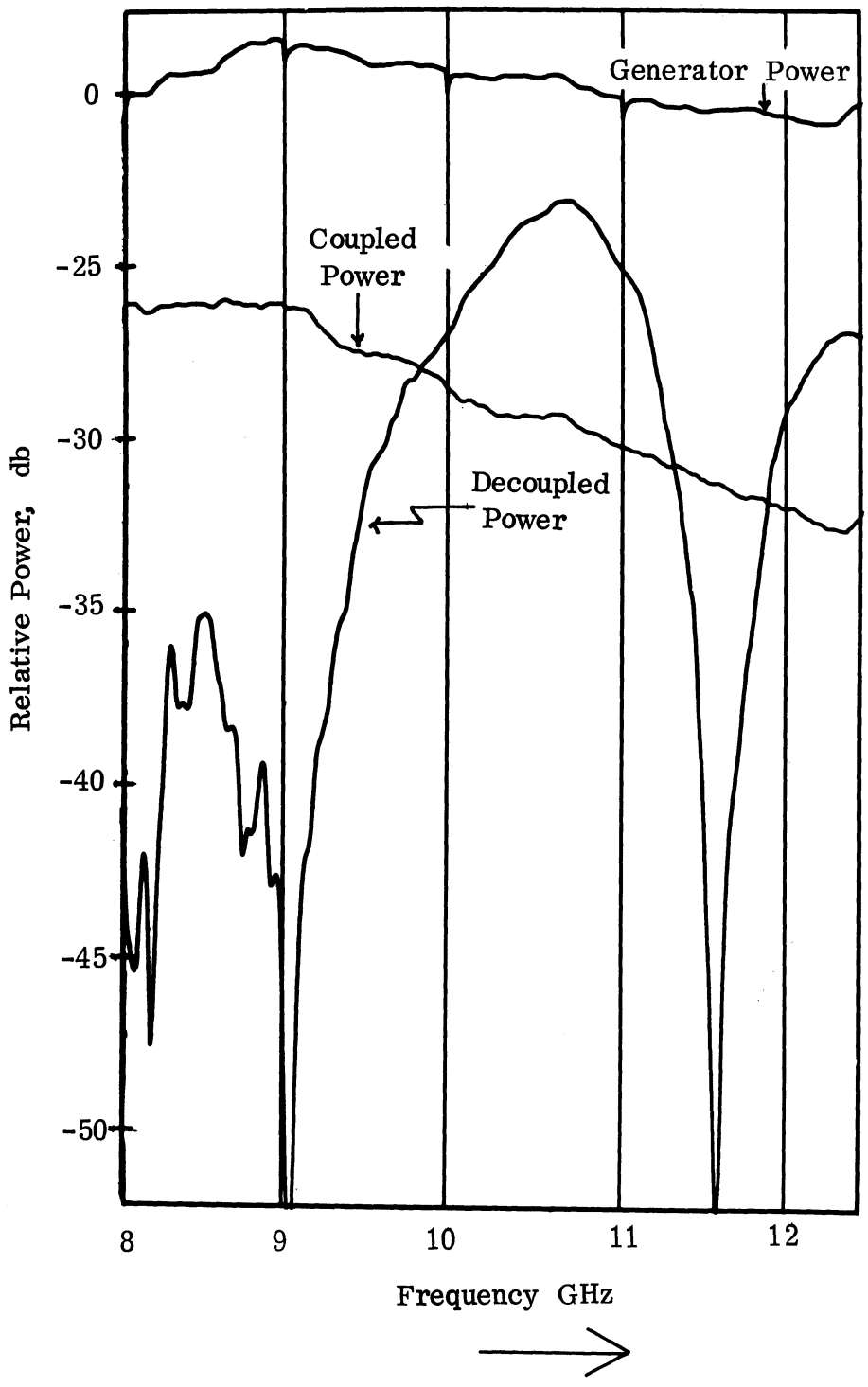

FIG. 2-22: DECOUPLING BY BRIDGE.

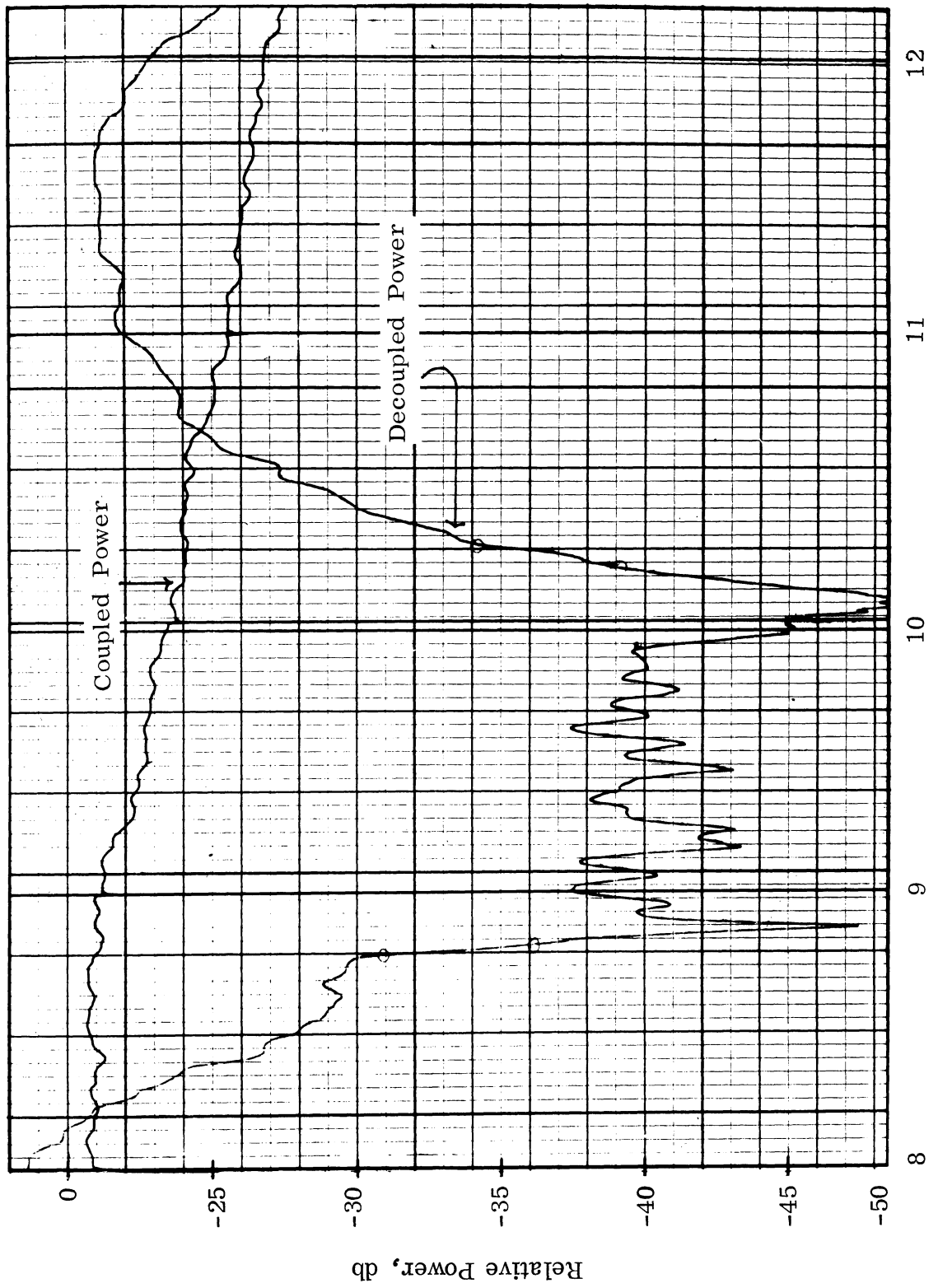

FIG. 2-23: DECOUPLING BY BRIDGE.

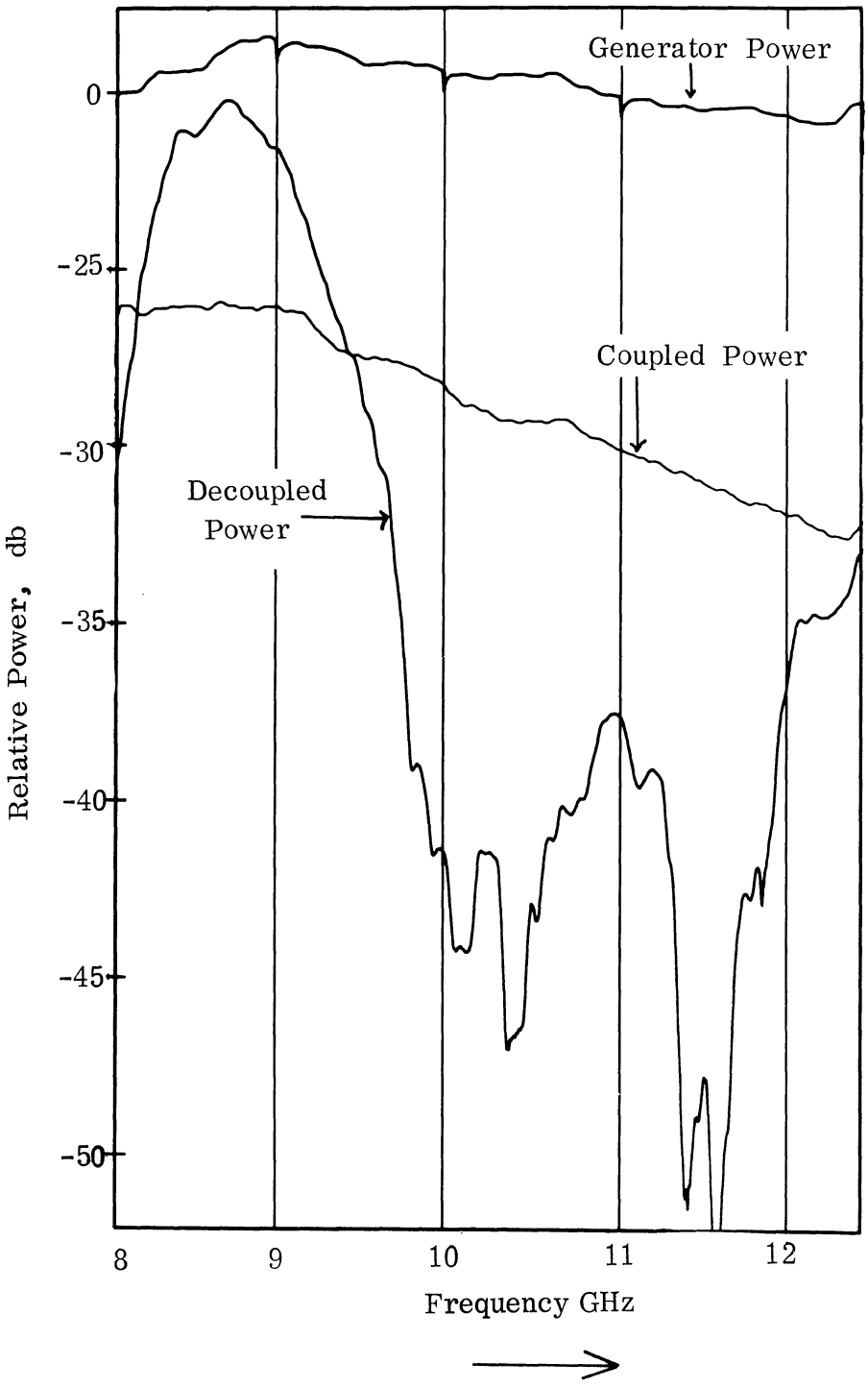

FIG. 2-24: DECOUPLING BY BRIDGE

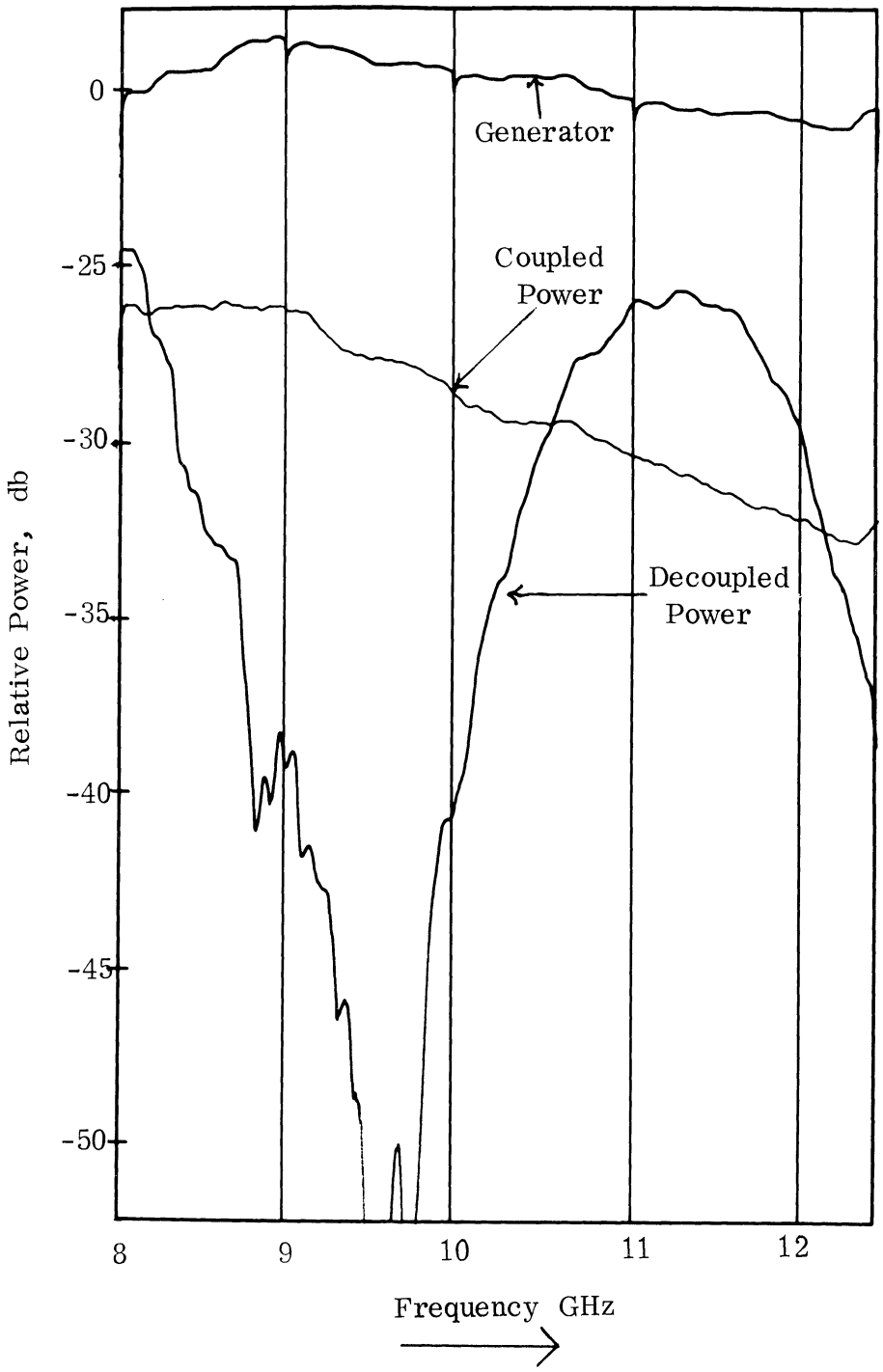

FIG. 2-25: DECOUPLING BY BRIDGE

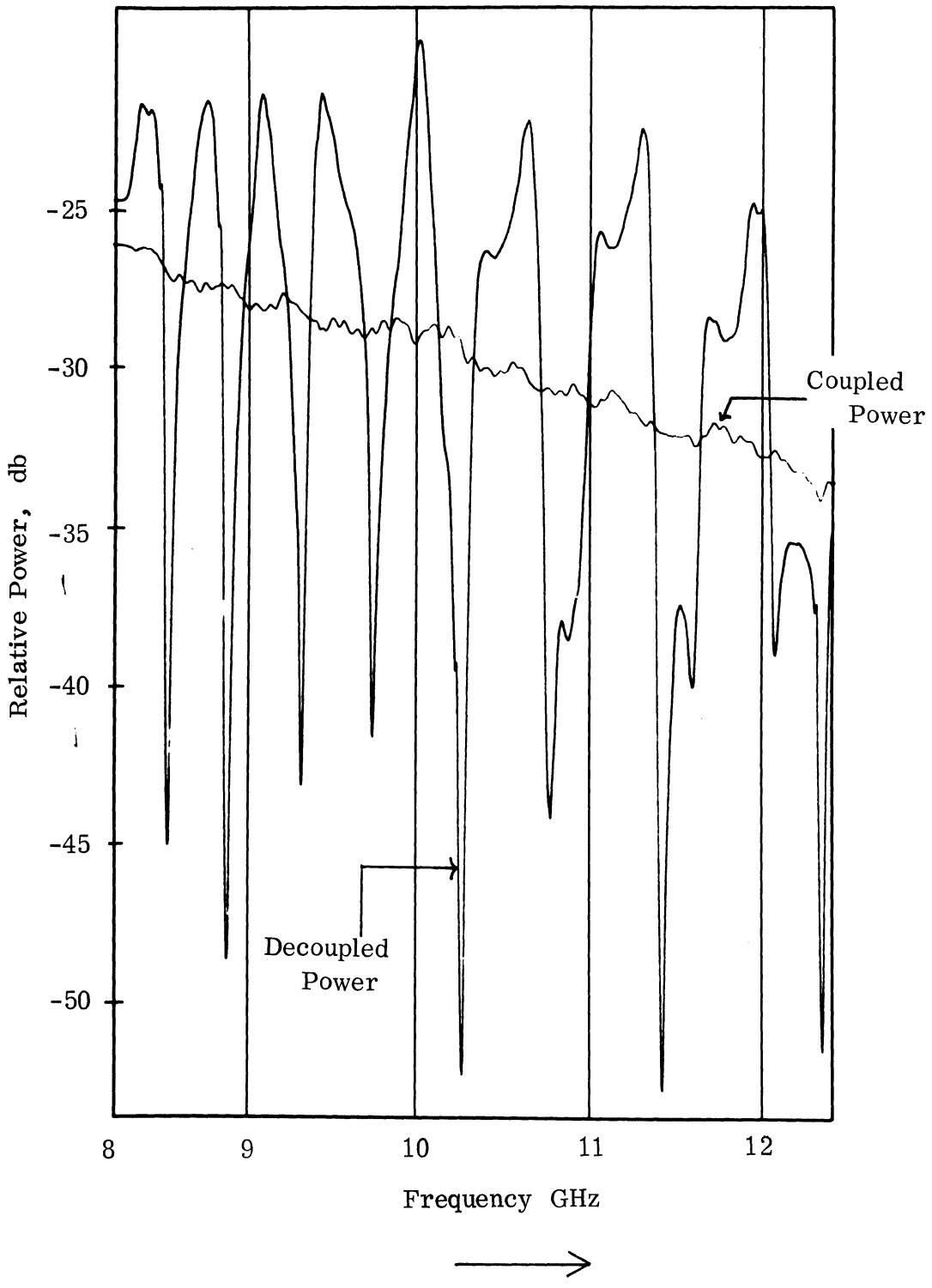

FIG. 2-26: DECOUPLING BY BRIDGE
(PATHS MISMATCHED)

air path produced a term in Eq. (2.13) which had a frequency dependent coefficient. One possible solution would be to place an equivalent air gap in the bridge path. This could be done with carefully aimed X-band horns, or with the proper length of air-line coax. This would produce a term involving an air path in Eq. (2.13) which might be made to cancel the term present now. This change would give a chance of obtaining very broadband decoupling.

The amount of decoupling obtained is dependent upon how well the amplitude of the bridge signal matches the amplitude of the coupled signal. If they were exactly equal, the decoupling expressed in db would be infinite. As the frequency is swept, however, the coupled power varies somewhat. Thus, to obtain more db's of decoupling, the bridge signal would have to match the variation of the coupled signal closely.

We also need to investigate the properties of the components used in our system. We need to know how the phase-shifter performs as a function of frequency. The attenuator α_2 has some phase-shift inherent in it too. Another thing to investigate is the length of the coupling path between slot A and slot B as a function of frequency. In general, the response of our system components must be known before any small irregularities can be compensated away.

A completely different idea is to achieve broadband decoupling by using two bridge paths and a filtering network. This is shown in Fig. 2-27. Bridge network 1 is set to null for the high frequencies; after passing through the high-pass filter the undesired adding in-phase at low frequencies is removed. Bridge network 2 is set to null at low frequencies; after passing through the low-pass filter the undesired adding in-phase at high frequencies is removed. The outputs of the two filters are added together, hopefully producing broadband decoupling.

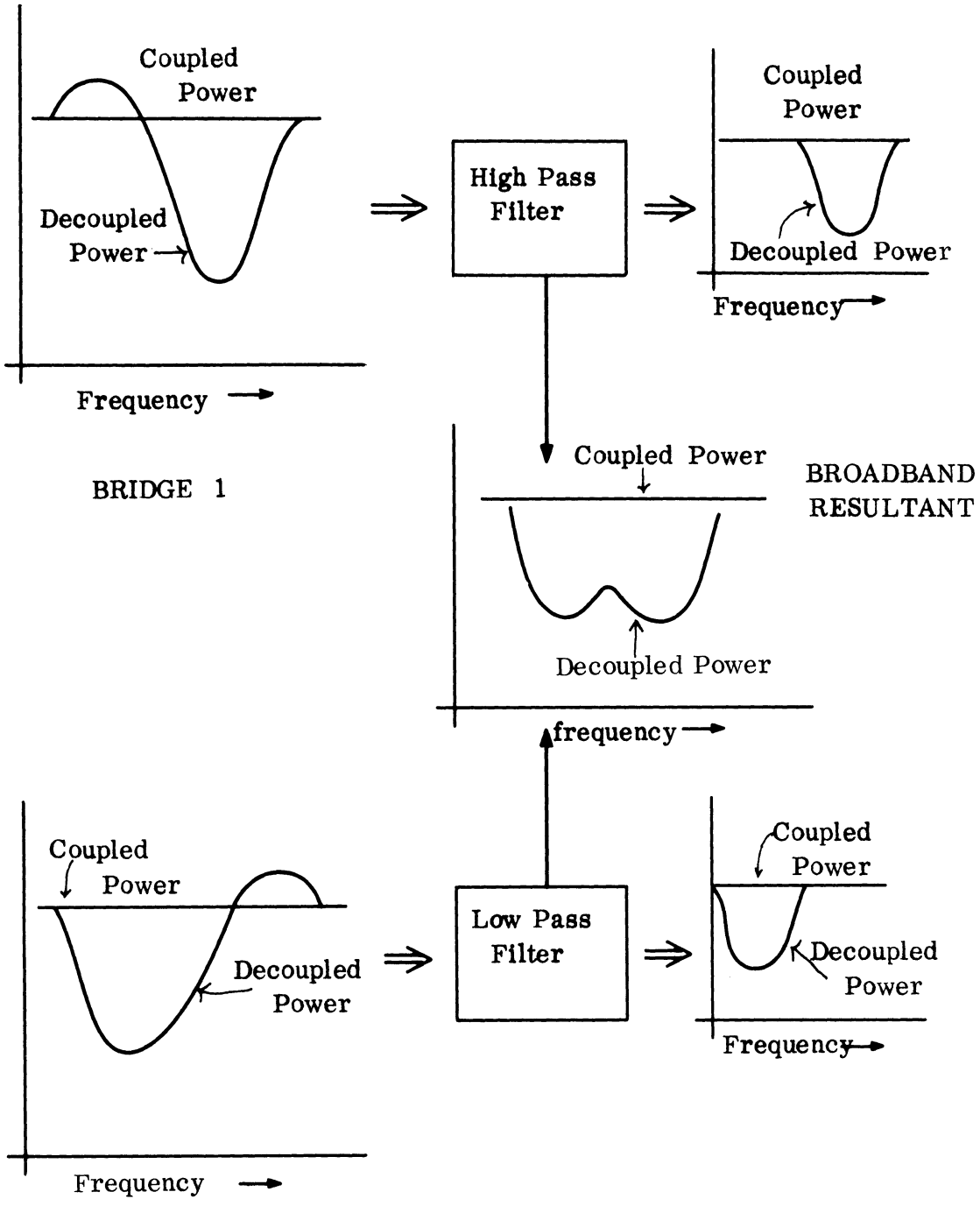

FIG. 2-27: BROADBANDING BY 2 BRIDGE LINKS WITH FILTERS

2.6 Coupling Between a Spiral and a Slot

A ground plane has been made for studying coupling and decoupling between S-band antennas such as slots, spirals and monopoles. Special attention was given to making some holes in the ground plane as closely together as possible so that the near field coupling effects can be included. As a preliminary work to future decoupling study, the coupling data between a spiral and a slot were obtained. The spirals used were two AFA circular Archimedean spirals and two Advanced Development Laboratories square Archimedean spirals. The arrangement of the antennas on the ground plane is shown in Fig. 2-28.

It is obvious from this figure that there are four factors affecting the value of coupling. These are:

1) The relative orientation of the slot with respect to a fixed spiral.

2) The center-to-center distance between the two antennas.

3) The azimuth angle ϕ or orientation of the spiral.

4) The frequency.

First consider the coupling along the two axes A-A and B-B which will be designated as the E-plane and H-plane coupling respectively. This should not be considered as inadequate to demonstrate the nature of the coupling since the coupling on the two axes are respectively the maximum and the minimum values and therefore yield the most informative data. Figures 2-29 to 2-32 show the results of circular spiral to slot coupling. Although the coupling was plotted as a function of ϕ with f and d as parameters, its dependence on f and d can readily be seen by comparing the data on different curves.

The effect of spiral orientation relative to the slot can be summarized. The E-plane coupling is seen to be stronger than H-plane coupling, especially for larger distances owing to the fact that the near field term is largely responsible for H-plane coupling.

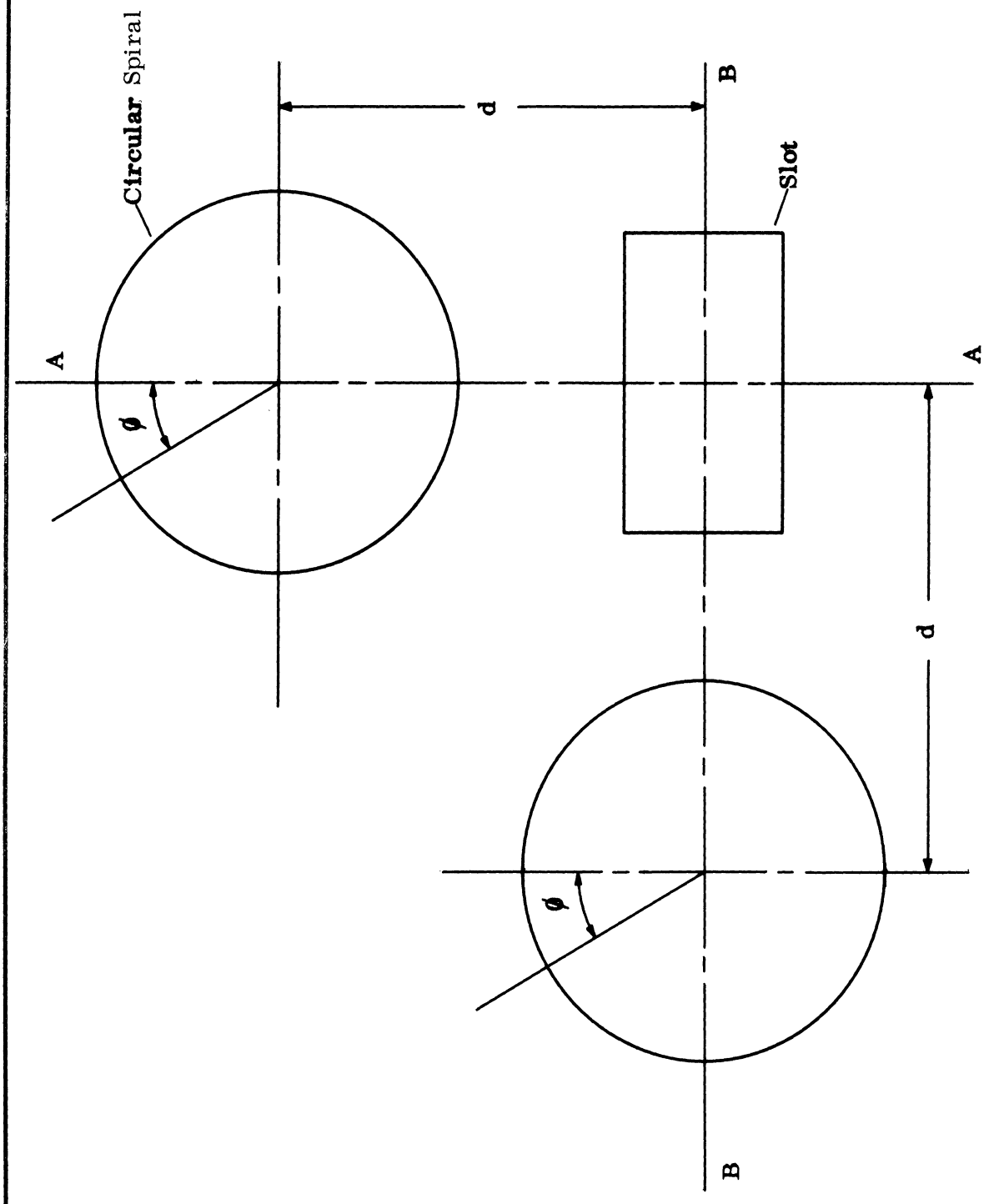

FIG. 2-28: GEOMETRY OF ANTENNAS ON THE GROUND PLANE.

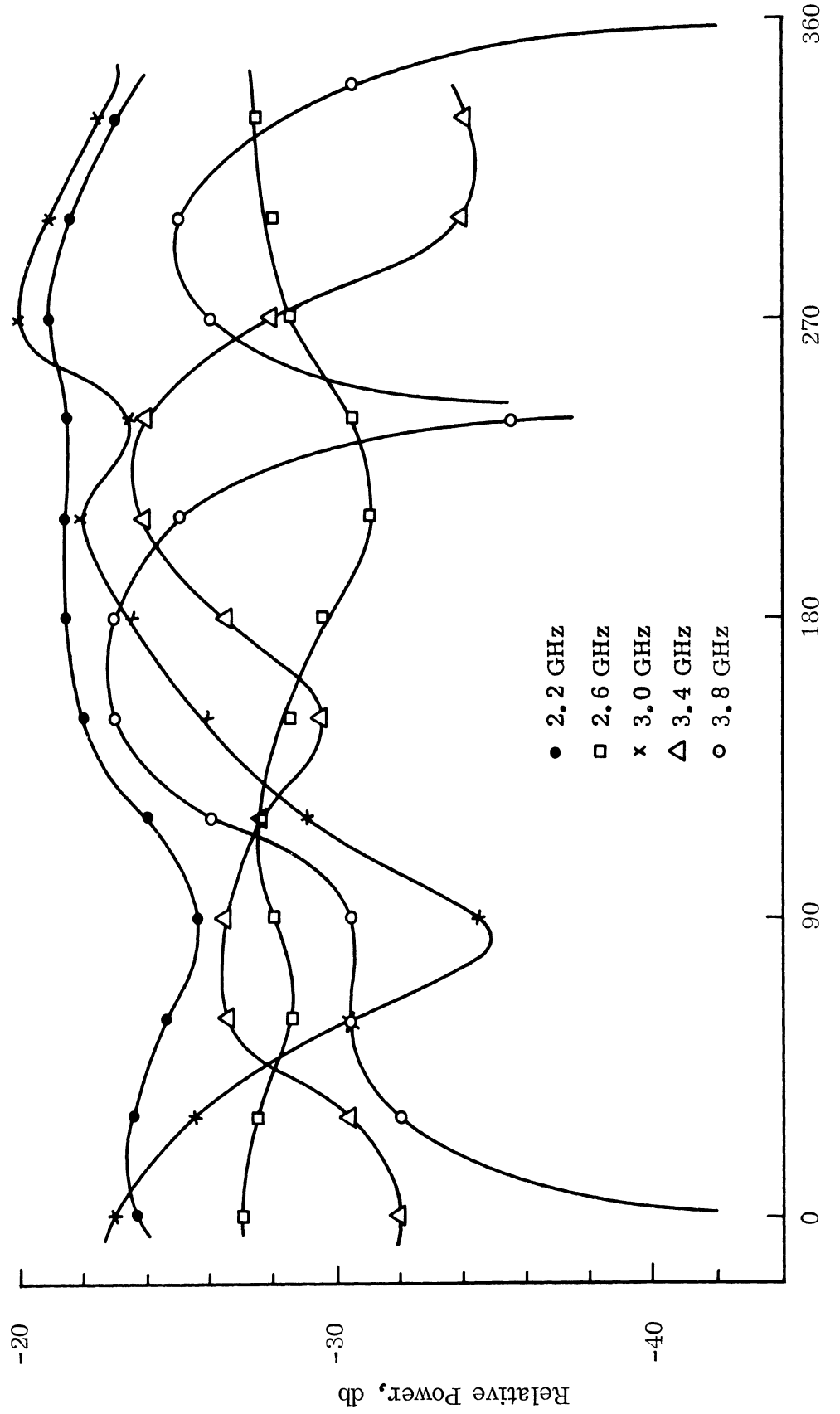

FIG. 2-29: E-PLANE COUPLING BETWEEN A CIRCULAR SPIRAL AND A SLOT VERSUS AZIMUTH ANGLE. (Center-to-center Distance 8.5 cm)

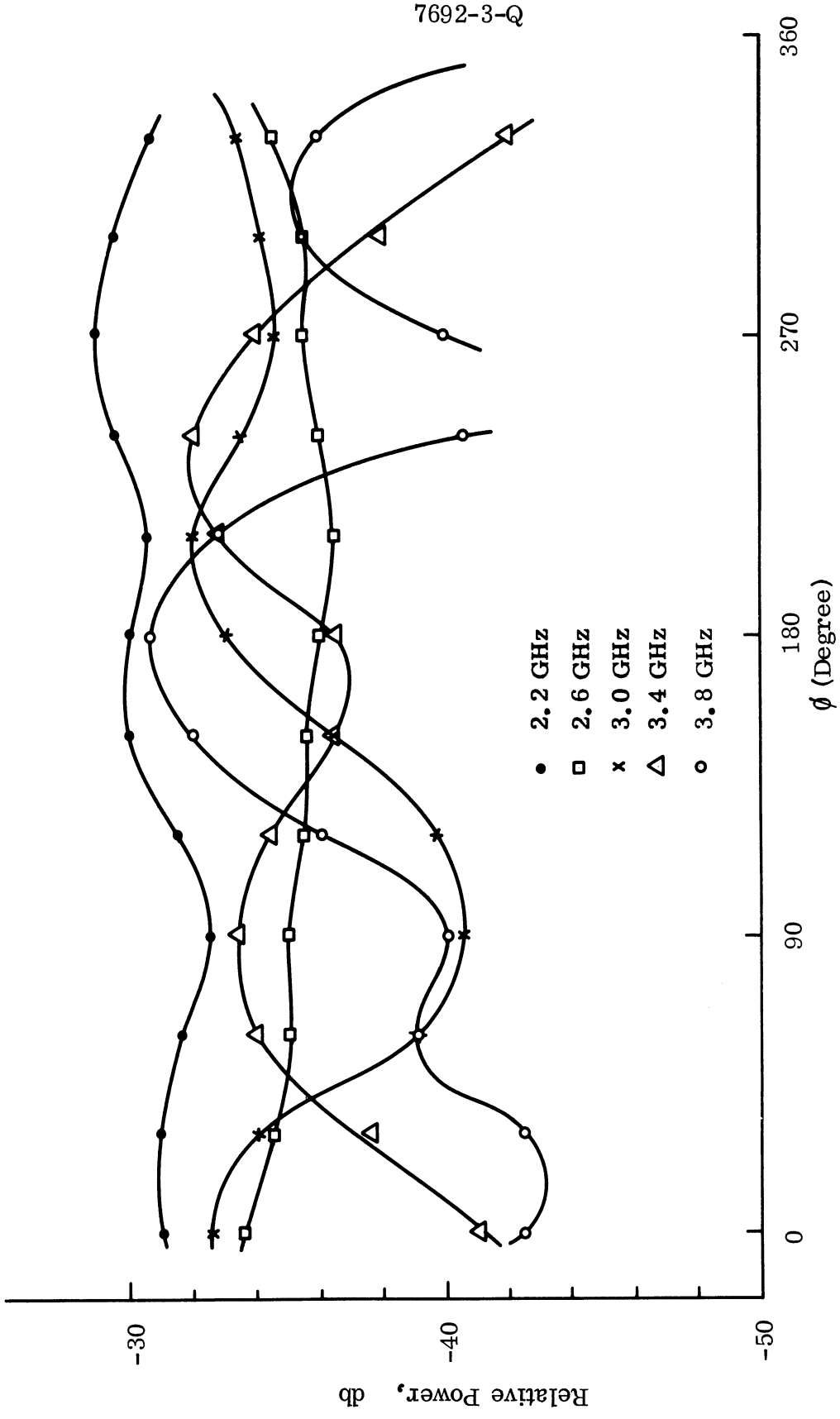

FIG. 2-30: E-PLANE COUPLING BETWEEN A CIRCULAR SPIRAL AND A SLOT VERSUS AZIMUTH ANGLE. (Center-to-center Distance 26 cm).

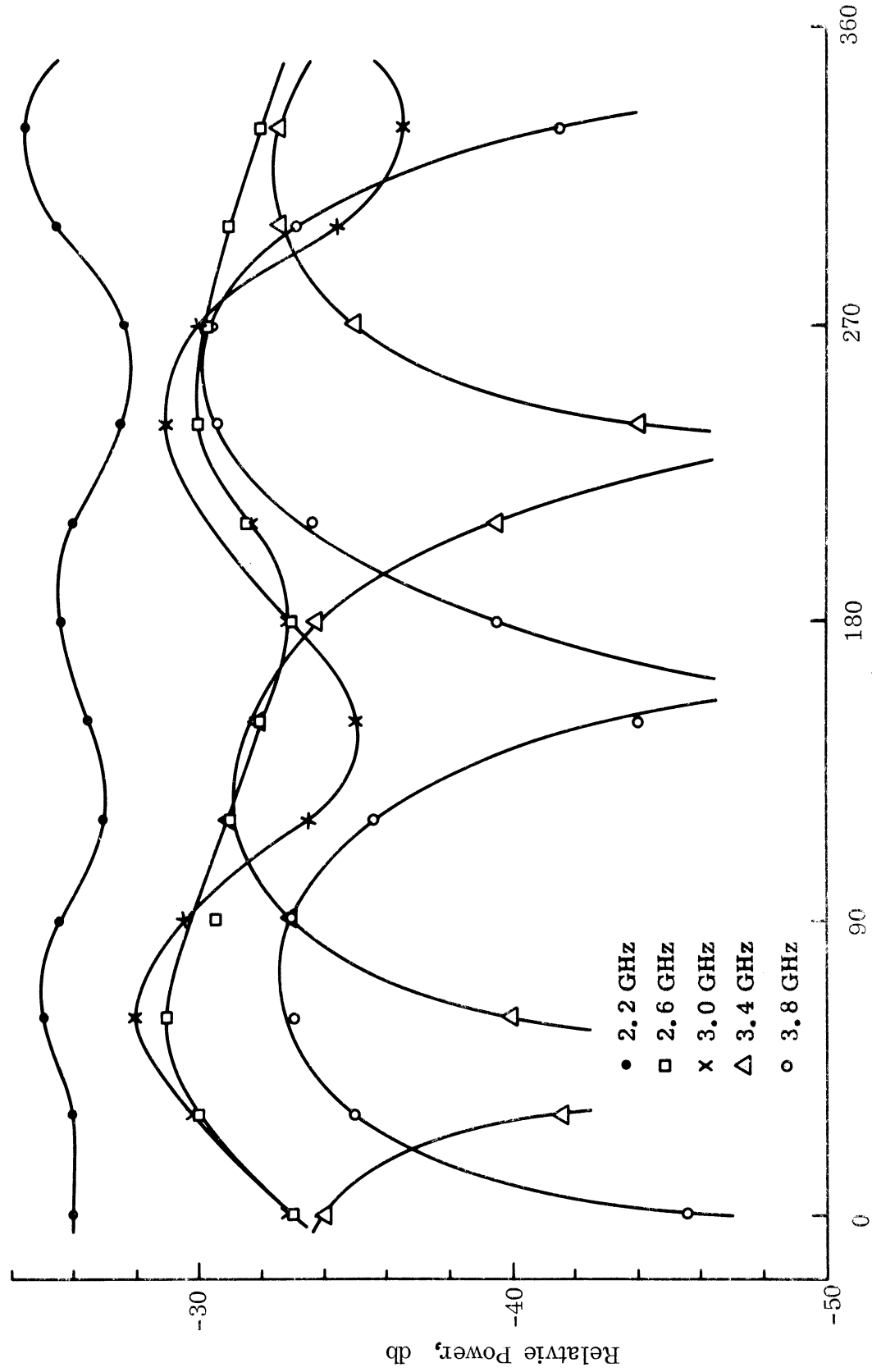

FIG. 2-31: H-PLANE COUPLING BETWEEN A CIRCULAR SPIRAL AND A SLOT VERSUS AZIMUTH ANGLE. (Center-to-center Distance 9.6 cm).

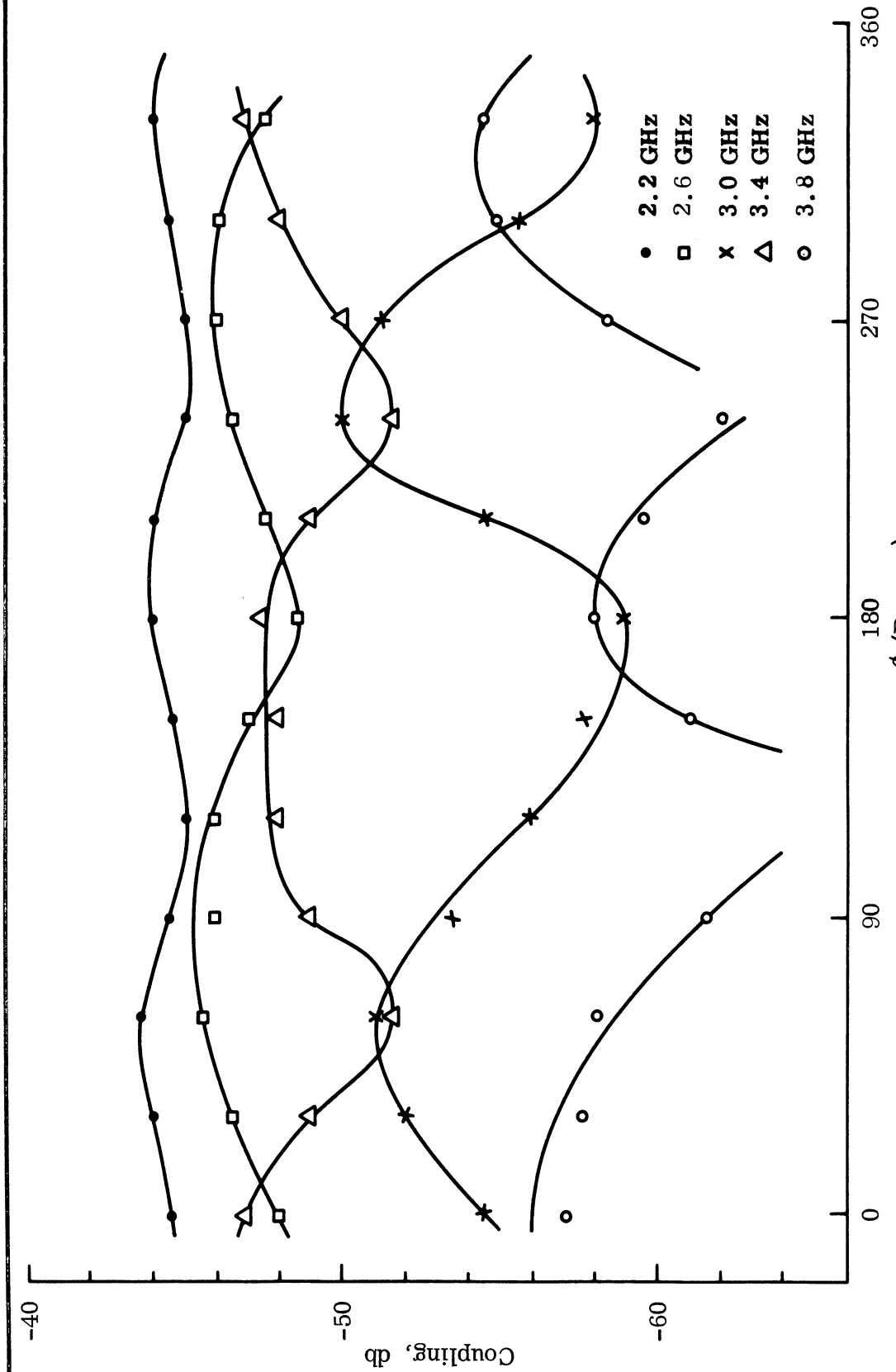

FIG. 2-32: H-PLANE COUPLING BETWEEN A CIRCULAR SPIRAL AND A SLOT VERSUS AZIMUTH ANGLE. (Center-to-center Distance 25.5 cm).

The ϕ variation of coupling is largely dependent on frequency. For 2.2 GHz and 2.6 GHz the variation is small; for 3.4 GHz and 3.8 GHz it is very large; for 3.0 GHz it is intermediate. This indicates clearly the influence of the less symmetrical structure of the spiral on coupling because the radiation region approaches the center of the spiral as the frequency goes up to the high frequency limit of the spiral. For 2.2 GHz and 2.8 GHz the radiation region has a radius about one-half that of the spiral. Good symmetry and small reflections from the end result in almost omnidirectional coupling.

The center-to-center distance and frequency dependence can be simply stated. These are intimately related. It is hard to draw any conclusion before normalizing to coupling versus wavelengths spacing. However, it is seen that the coupling does not follow the far field 6 db per octave rule for both E-plane and H-plane coupling. Most of the features in the spiral-to-slot coupling are not unlike those previously published by this project group on spiral-to-monopole coupling. For an interesting comparison, the reader is referred to earlier reports (J.A.M. Lyon, et al, 1966).

III

ABSORBING MATERIALS

In this report magnetic loss tangent and magnetic Q data are included completing a twelve sample series (Fig. 3-1 through 3-5). The frequency range where measurements were taken necessitated the determination of the μ' and μ'' parameters by the use of an impedance bridge and a sample holder shorted at one end with the specimen in contact with the short termination.

Ideally if the sample is placed in the position where the electric field is maximum, or at $\lambda/4$ away from the short termination one should be able to determine ϵ' and ϵ''. However, due to the fact that one is unable to obtain with this technique reproducible results at the particular frequency range of 50 - 400 MHz the data obtained on ϵ' and ϵ'' are not reported. Concurrently with the above effort, measurements are taken now at frequencies between 2000 - 7000 MHz. The technique used for this particular range of frequencies is that of the determination of the propagation constant γ and intrinsic impedance of the specimen through the determination of open and short circuit impedance measurements with the sample in a coaxial line. This method appears to be the most accurate one used so far since corrections compensate for the residual VSWR on the line and the noise level. A computer program is available for the calculations.

From the information presented in this report one may deduce that some of the mixtures present a high absorbing capacity. Of particular notice is mixture 2 which has both broadband characteristics and high magnetic loss tangent between 50 and 400 MHz as can be seen in Fig. 3-2b. A complete chart of the data appears in Table IV-1.

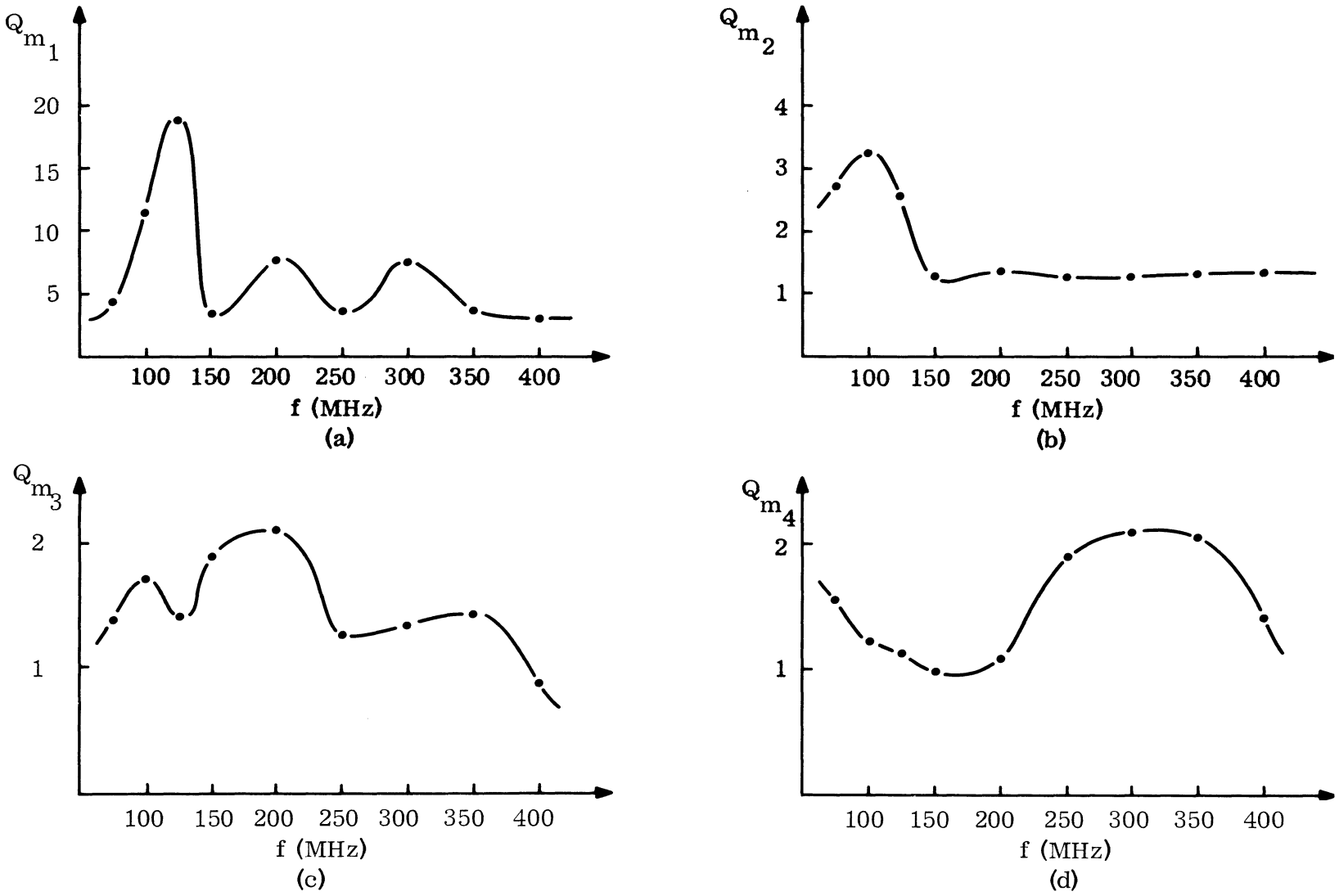

FIG. 3-1: SPECIMEN MAGNETIC Q VERSUS FREQUENCY.

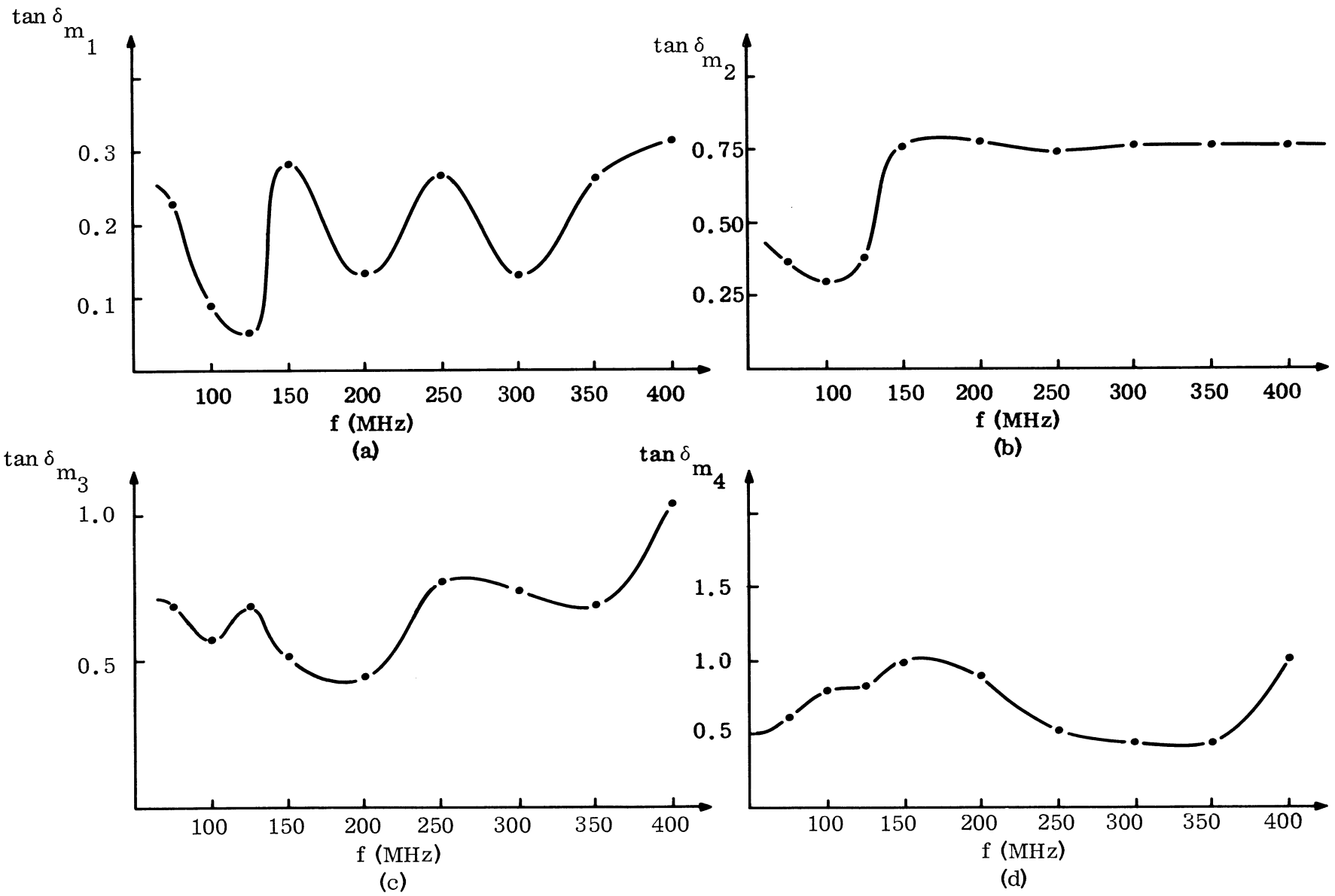

FIG. 3-2: SPECIMAN LOSS TANGENT VERSUS FREQUENCY

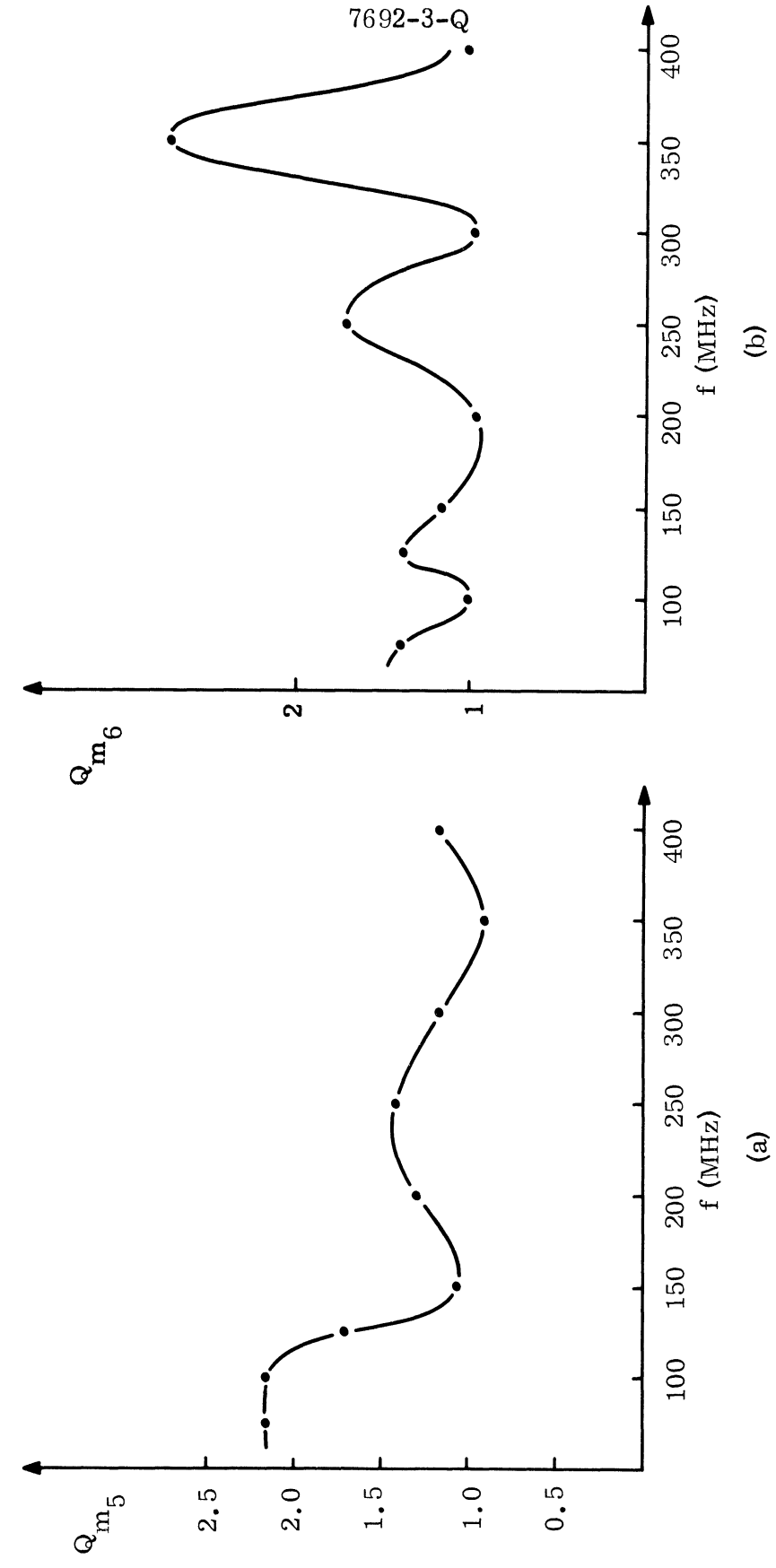

FIG. 3-3: SPECIMEN MAGNETIC Q-FACTOR VERSUS FREQUENCY.

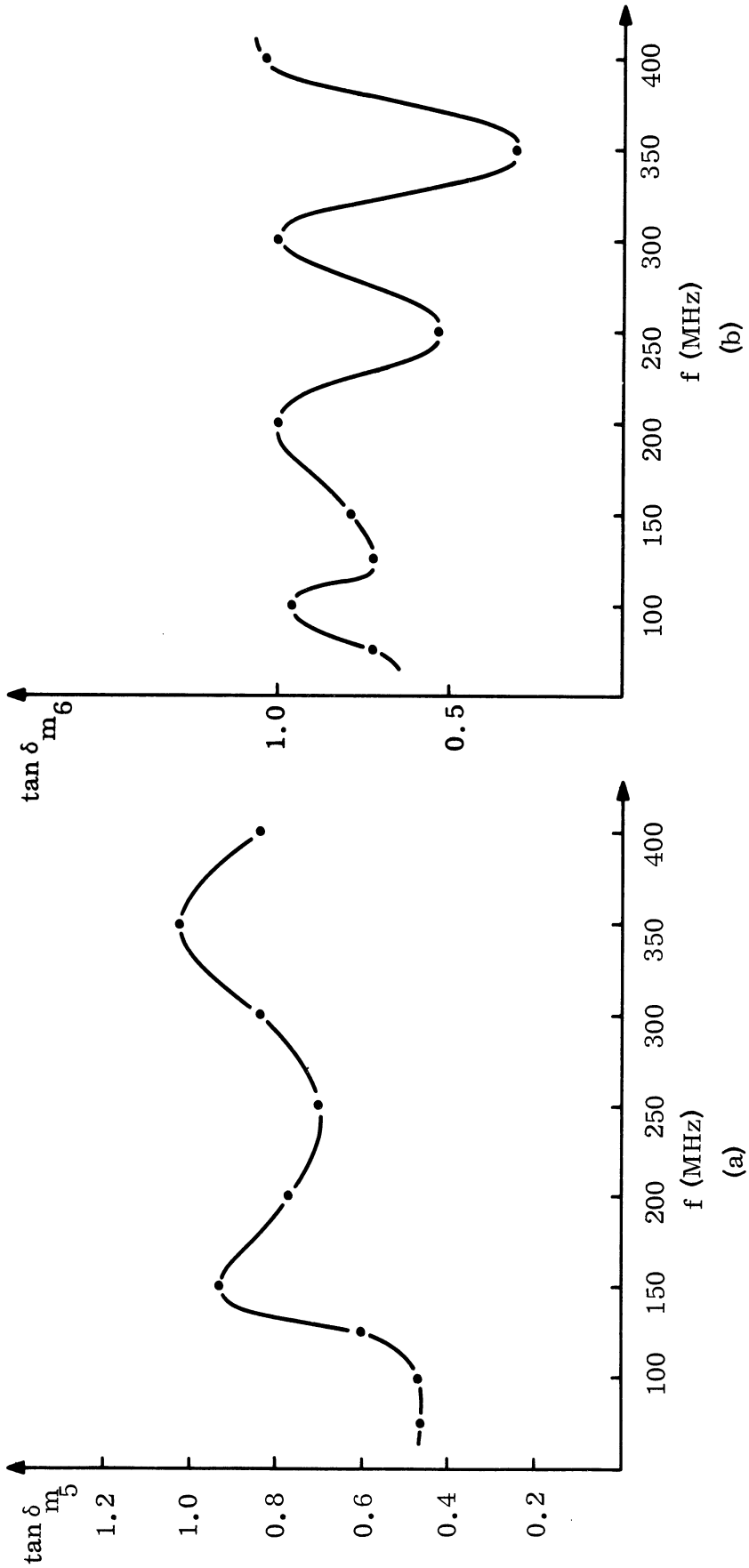

FIG. 3-4: SPECIMEN MAGNETIC LOSS TANGENT VERSUS FREQUENCY.

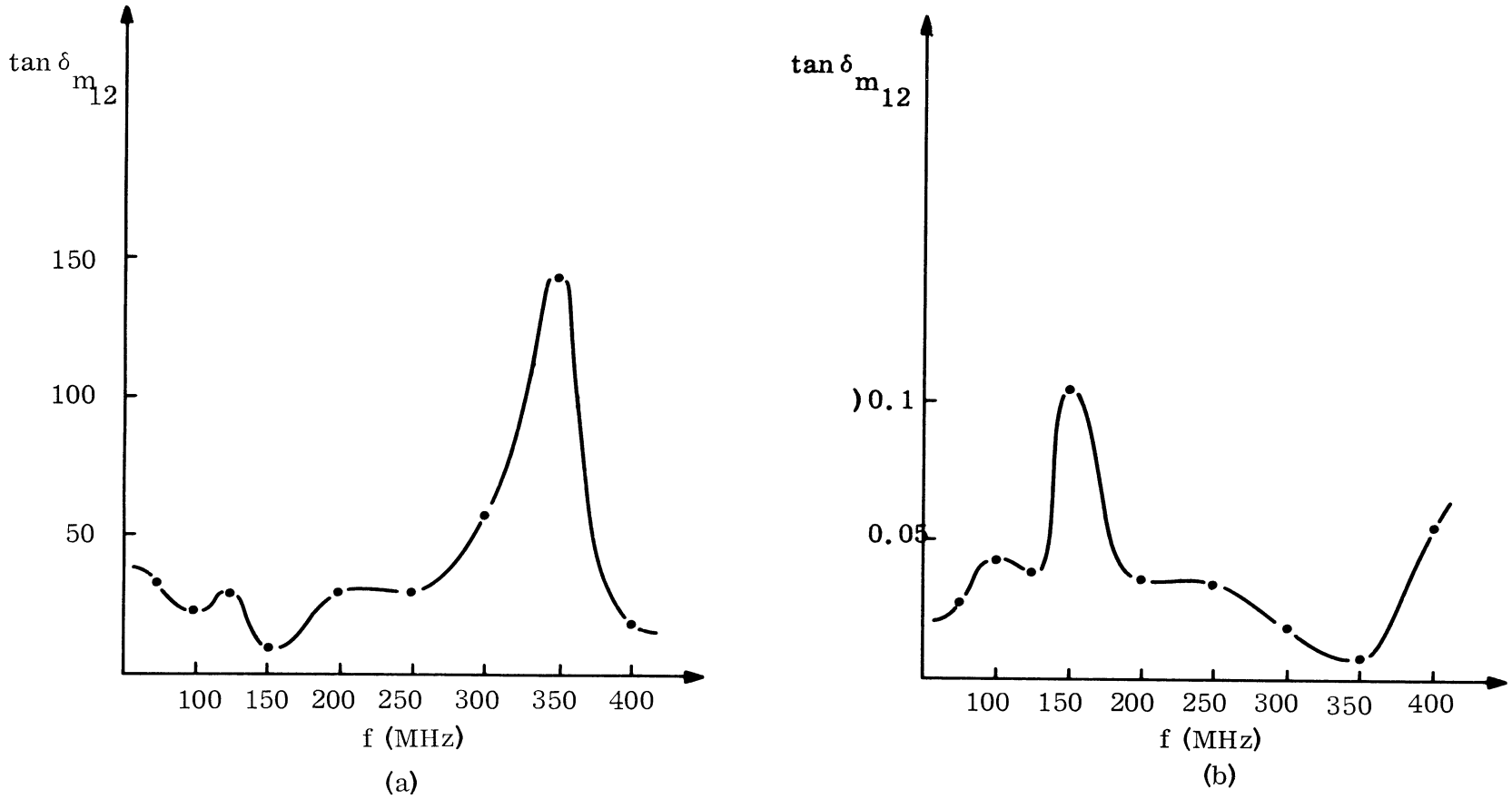

FIG. 3-5: (a) MAGNETIC Q VERSUS FREQUENCY, (b) MAGNETIC LOSS TANGENT VERSUS FREQUENCY.

TABLE III-1

f (MHz)	Q_{m_1}	$\tan\delta_{m_1}$	Q_{m_2}	$\tan\delta_{m_2}$	Q_{m_3}	$\tan\delta_{m_3}$	Q_{m_4}	$\tan\delta_{m_4}$	Q_{m_5}	$\tan\delta_{m_5}$	Q_{m_6}	$\tan\delta_{m_6}$	$Q_{m_{12}}$	$\tan\delta_{m_{12}}$
75	4.5	0.222	2.74	0.365	1.43	0.7	1.57	0.636	2.15	0.465	1.43	0.7	33.6	0.0298
100	11.4	0.097	3.27	0.306	1.73	0.578	1.25	0.8	2.15	0.465	1.07	0.935	22.9	0.0437
125	19.2	0.052	2.6	0.385	1.43	0.7	1.19	0.84	1.73	0.6	1.425	0.7	28.6	0.035
150	3.49	0.286	1.3	0.77	1.92	0.522	1.0	1.0	1.07	0.935	1.2	0.834	9.5	0.105
200	7.62	0.131	1.28	0.775	2.14	0.468	1.1	0.91	1.3	0.768	1.0	1.0	28.6	0.035
250	3.72	0.269	1.29	0.753	1.28	0.78	1.92	0.52	1.425	0.7	1.735	0.577	28.75	0.0346
300	7.65	0.130	1.3	0.77	1.33	0.752	2.14	0.467	1.19	0.84	1.0	1.0	57.2	0.0174
350	3.74	0.268	1.3	0.77	1.43	0.7	2.14	0.467	0.921	1.087	2.75	0.363	143	0.007
400	3.18	0.315	1.3	0.77	0.87	1.145	0.919	1.08	1.19	0.84	0.912	1.095	19.15	0.056

IV

CONCLUSIONS

The work effort during this report period has indicated promising improvement of isolation obtained over what was reported for the previous quarter. The 15 db of isolation acquired through the use of a bridge link, good for 1.5 GHz bandwidth coverage for the X-band, is indeed promising. However, the use of absorbing material with E-Sectoral Horns providing 18 db of isolation system to system over X-band is also encouraging. Circumferential chokes around a driven slot or an active slot giving 22 db system-to-system over 0.5 GHz can offer a useful isolation increase if this narrow bandwidth coverage is satisfactory for X-band. The same method offers 14 db increased isolation over the entire X-band.

The work reported on corrugations is still preliminary. Much needs to be done to make corrugations provide a satisfactory increase of isolation. Likewise, the use of parasitic slot elements has brought on a system-to-system basis an increase of 7 db over 2.5 GHz for X-band.

The decoupling results are summarized in Table IV-1 of this section. This table enables a simple comparison to be made of the various methods. In actual use of methods to combat a known system-to-system interference problem, it is quite likely that more than one of the several methods will be needed to bring the offending signal down to an appropriate level.

It is to be observed in this table that proper initial orientation of antennas within the limitations of polarization and direction requirements of the antennas affords a very useful means of introducing isolation between two systems. The other methods in the table are by their nature suited to modifications. However, the initial antenna orientation is one dictated by the design requirements for operation of the systems involved. All coupling reduction techniques are adaptable to systems operating at various frequency bands.

Isolation Method	Antennas Used	System Isolation Increase in db[+]	Bandwidth[++]	Side Effects
Antenna Orientation	Slots, E- and H-Sectoral Horns	At least 40[+++]	X-band	None
RF Bridge	Slots	15	1.5 GHz	Up to 5 db isolation decrease for higher and lower frequencies.
Antennas Recessed in Cavity Partially Filled With Absorber	E-Sectoral Horn	18 db	X-band	Up to 0.6 db loss in maximum gain[++++]
	Slots	13 db	X-band	Up to 1 db increase in maximum gain Half-power beamwidth reduced.
Circumferential Chokes	Slots	22 db	0.5 GHz	Up to 4 db increase in maximum gain
		14 db	X-band	Half-power beamwidth reduced.
Corrugations	Slots	5 db	X-band	Assymmetrical radiation pattern with 2 db troughs within $\pm 30^{o}$ of broadside.
Parasitic Antenna	Slots	7 db	2.5 GHz	Assymmetrical radiation pattern.

TABLE IV-1: SUMMARY OF DECOUPLING METHODS AND RESULTS. (ALL STRUCTURES ARE FLUSH-MOUNTED.)

[+] For E-plane coupling

[++] All experiments conducted in X-band (8.2 - 12.4 GHz)

[+++] Theoretically infinite.

[++++] (Gain) = (Directivity) x (Efficiency)

The various methods of increasing decoupling or increasing isolation that have been studied in this report have been made with full cognizance of the undesirability of modifying the radiation characteristics of the antennas involved. For this reason, experimental data have been shown indicating to some extent the limitations imposed on the radiation pattern of an antenna by the influence of absorber or surface modifications.

V

FUTURE EFFORT

During the next report period, it is anticipated that extensive work will be done on the bridge link method which has been described in this report. It is expected that additional bridge links will be utilized each, one covering a given bandwidth. By the use of several links, each with its own filtering, it is expected that the entire X-band could be covered by this method.

The methods using absorber will benefit by the purchase of different types of absorber and by the use of absorber which has been fabricated on this project. The fabrication of absorber on this project has been limited to readily mixed materials having the desired electrical characteristics. It is expected that isolation by either chokes or corrugations will be improved both in magnitude and bandwidth by the use of appropriate absorbing material.

ACKNOWLEDGMENTS

Mr. D.R. Brundage of The University of Michigan, Institute of Science and Technology, obtained most of the experimental data in this report.

REFERENCES

Coe, R.J. and Held, G. (January, 1964), "A Parasitic Slot Array," IEEE Trans., AP-12, No. 1, pp. 10-16.

Hurd, R.A. (December, 1954), "The Propagation of an Electromagnetic Wave Along an Infinite Corrugated Surface," Can. J. Phys., 32, No. 12, pp. 727-734.

Kraus, J.D. (1950), Antennas, McGraw-Hill Book Company.

Lyon, J.A.M., Kalafus, R.M., et al (April, 1966), "Derivation of Aerospace Antenna Coupling-Factor Interference Prediction Techniques," The University of Michigan Radiation Laboratory, Technical Report AFAL-TR-66-57.

Lyon, J.A.M., et al (May, 1966), "Electromagnetic Coupling Reduction Techniques," The University of Michigan Radiation Laboratory, Report 7692-2-Q.

THE UNIVERSITY OF MICHIGAN

DISTRIBUTION LIST

	No. of Copies
Aerospace Corporation Attn: Mr. Robert G. Hansen 2400 E. El Segundo Blvd Los Angeles, California 90045	1
Andrew Alfred Consulting Engineers Attn: Librarian (Antenna Section) 299 Atlantic Avenue Boston, Massachusetts 02110	1
AVCO Corporation Research and Advanced Development Division Attn: Research Library 201 Lowell Street Wilmington, Massachusetts 01887	1
Bell Telephone Laboratories, Inc Attn: Technical Reports Librarian Room 2A 165 Whippany, New Jersey 07961	1
Bendix Corporation Research Laboratories Division Attn: Mr. G. M. Peach 20800 10 1/2 Mile Road Southfield, Michigan 48076	1
Boeing/Headquarters Aerospace Division Attn: Technical Library M/F Antenna and Radomes Unit P.O. Box 3707 Seattle, Washington 98124	1
Collins Radio Corporation Attn: Dr. Robert L. Carrel Antenna Section Dallas, Texas 75207	1

(continued)

DISTRIBUTION LIST
(continued)

Douglas Aircraft Company, Inc
Attn: MSSD Technical Library
(Antenna Section)
3000 Ocean Park Blvd
Santa Monica, California 90406 1

General Dynamics/Fort Worth Division
Attn: Technical Library
(Antenna Section)
Grants Lane, P.O. 748
Fort Worth, Texas 76101 1

General Electric Company
Electronics Laboratory
Attn: Technical Library
Electronics Park
Syracuse, New York 13201 1

Hughes Aircraft Corporation
Attn: Technical Library
(Antenna Section)
Centinela and Teale Streets
Culver City, California 90232 1

ITT/Federal Laboratories
Attn: Technical Library
(Antenna Section)
500 Washington Avenue
Nutley, New Jersey 07110 1

Ling-Tenco-Vought
Military Electronic Division
Attn: Librarian (Antenna Laboratory)
1200 Jupiter Street
Garland, Texas 75222 1

(continued)

DISTRIBUTION LIST
(continued)

Lockheed Aircraft Corporation
Electronic and Armanents System Office
P.O. Box 551
Burbank, California 91503 1

The Martin/Denver
Division Headquarters
Attn: Antenna Laboratory Mail Mr
T-0453 P.O. Box 179
Denver, Colorado 80201 1

McDonnell Aircraft Corporation
Attn: Technical Library
(Antenna Section)
Box 516
St. Louis, Missouri 63166 1

Motorola, Inc
Western Military Electronics Division
8201 E. McDowell
Scottsdale, Arizona 1

North American Aviation, Inc
Attn: Technical Library
(Engineering Dept)
4300 E. Fifth Avenue
Columbus, Ohio 43216 1

Radio Corporation of America
Missile and Service Radar Division
Attn: Manager, Antenna Engineering
Skill Center
Marne Highway
Moorestown, New Jersey 08057 1

Raytheon Company
Space and Information Systems Division
Attn: Antenna Group
P.O. Box 1542
Goleta, California 93017 1

(continued)

DISTRIBUTION LIST
(continued)

Space Technology Laboratory
Attn: Research Library
One Space Park
Redondo Beach, California 90278 — 1

Stanford Research Institute
Attn: Librarian (Antenna Laboratory)
Ravenwood Street
Menlo Park, California 94025 — 1

Sylvania Electronics Systems Division
Attn: Librarian (M/F Antenna and
Microwave Laboratory)
40 Sylvan Street
Waltham, Massachusetts 02154 — 1

Westinghouse Electric Corporation
Aerospace Division
P.O. Box 746
Baltimore, Maryland 21203 — 1

GOVERNMENT

AFAL (AVWE-3)
Wright-Patterson AFB
Ohio 45433 — 6

SEG (SEAFM - Mr. Mulligan)
Wright-Patterson AFB
Ohio 45433 — 1

SEG (SEPIE)
Wright-Patterson AFB
Ohio 45433 — 1

AFCRL (CRD - Mr. C. J. Sletton)
L. G. Hanscom Field
Bedford, Massachusetts 01731 — 1

(continued)

DISTRIBUTION LIST
(continued)

AFETRL (Technical Library)
Patrick AFB
Florida 32925 — 1

AFMDC (Technical Library)
Holloman AFB
New Mexico 88330 — 1

RADC (EMTLT - 1)
Griffiss AFB
New York 13442 — 1

ESD/ESRRE
L.G. Hanscom Field
Bedford, Massachusetts 01731 — 1

HTD/RTTC
Bolling AFB
Washington D.C. 20330 — 1

USAF AFRST/Major Jaffers
Washington D. C. 20330

OAR Building T-3
Washington D. C. 20333 — 1

RADC/EMCRV
Griffiss AFB
New York 13442 — 1

ASD (AVS)
Wright-Patterson AFB
Ohio 45433 — 1

ASD (ASZFT)
Wright-Patterson AFB
Ohio 45433 — 1

DISTRIBUTION LIST
(continued)

ASD (ASZIE) Wright-Patterson AFB Ohio 45433	1
ASD (ASZW) Wright-Patterson AFB Ohio 45433	1
ASD (ASTFP) Wright-Patterson AFB Ohio 45433	1
SEG (SEACR) Wright-Patterson AFB Ohio 45433	1
AFIT Wright-Patterson AFB Ohio 45433	1
Electromagnetic Compatibility Analysis Center Code ACG U.S. Navy Marine Engineering Laboratory Anapolis, Maryland 21402	1
Electromagnetic Compatibility Analysis Center Code ACZ U.S. Navy Marine Engineering Laboratory Anapolis, Maryland 21402	1
Electromagnetic Compatibility Analysis Center Code ACO U.S. Navy Marine Engineering Laboratory Anapolis, Maryland 21402	1
RADC (EMATA) Griffiss AFB New York 13442	1

(continued)

DISTRIBUTION LIST
(c0ntinued)

RADC (EMIAD - Mr. R. F. Davis)
Griffiss AFB
New York 13442 — 1

AFSC (SCSE)
Andrews AFB
Washington D. C. 20330 — 1

Hq USAF (AFRDRE - Lt Col B. Lieber)
Washington D. C. 20330 — 1

Hq USAF (AFISAI)
Air Battle Analysis Center
Deputy Director of Plans for War Plans
Directorate of Plans DCS/PandO
Washington D. C. 20330 — 1

Office of Asst Secretary of Defense (FAD)
Technical Library
Room 3E 1065, The Pentagon
Washington D. C. 20330 — 1

RTD (RTTR)
Bolling AFB
Washington D. C. 20332 — 1

USAFSS (ESD/ESG - Mr. A. Martines)
San Antonio, Texas 78241 — 1

Commanding Officer
USAERDL (Attn: SIGRA/NAI)
Fort Monmouth, New Jersey 07703 — 1

Commanding General
US Army White Sands Missile Range
Attn: Technical Library RR-312
White Sands, New Mexico 88002 — 1

(continued)

DISTRIBUTION LIST
(continued)

Commanding Officer Harry Diamond Laboratories Conn Avenue and Vann Ness Streets, NW Attn: 240 Washington D.C. 20433	1
NASA Goddard Space Flight Center Attn: Antenna Branch - Mr. Lantz Code 525 Greenbelt, Maryland 20771	1
Director Naval Research Laboratory Attn: Code 5200 Washington D. C. 20390	
Commander U.S. Naval Test Center Attn: WSST-54, Antenna Section Patuxent River, Maryland 20910	1
Director US Navy Electronics Laboratory Code 3220 Attn: Library San Diego, California 92152	1
DDC Cameron Station Alexandria, Virginia 22314	20 + card
AUL (3T-AUL-59-30) Maxwell AFB Alabama 36112	1

(continued)

DISTRIBUTION LIST
(continued)

Vicent DeSanti, Chief
Exchange Section
Document Control Section
Scientific and Technical
Information Facility
P. O. Box 5700
Bethesda, Maryland 1

RTD (RTGS)
Bolling AFB
Washington D. C. 20332 1

FTD (TDEE)
Wright-Patterson AFB
Ohio 45433 1

UNIVERSITIES

Cornell Aeronautical Laboratory
Attn: Research Library
Buffalo, New York 14221 1

Georgia Institute of Technology
Engineering Experiment Station
Attn: Technical Library
M/F Electronics Division
Atlanta, Georgia 30313 1

Johns Hopkins University
Carlyle Barton Laboratory
Charles and 34th Streets
Baltimore, Maryland 22218 1

Lincoln Laboratories
Massachusetts Institute of Technology
Attn: Document Room P.O. Box 73
Lexington, Massachusetts 02173 1

(continued)

DISTRIBUTION LIST
(continued)

Ohio State University Research Foundation Attn: Technical Library (M/F Antenna Lab) 2024 Neil Avenue Columbus, Ohio 43210	1
Polytechnical Institute of Brooklyn Attn: Professor A. A. Oliner Microwave Research Institute 55 Johnson Street Brooklyn, New York 11201	1
Stanford Electronic Laboratory Attn: Librarian (Antenna Laboratory) Stanford, California 94025	1
Syracuse University Electrical Engineering Department Attn: Dr. Jose Perihi Syracuse, New York 13210	1
University of Southern California EE Department, Mr. W. V. Trusch University Park Los Angeles, California 90007	1
The University of Michigan Radiation Laboratory, Dept. of EE. R. E. Hiatt 201 Catherine Street Ann Arbor, Michigan 48108	1

Total 100 copies

UNCLASSIFIED

Security Classification

DOCUMENT CONTROL DATA - R&D

(Security classification of title, body of abstract and indexing annotation must be entered when the overall report is classified)

1. ORIGINATING ACTIVITY (Corporate author) The University of Michigan Radiation Laboratory Department of Electrical Engineering	2a. REPORT SECURITY CLASSIFICATION Unclassified 2b. GROUP

3. REPORT TITLE

Electromagnetic Coupling Reduction Techniques

4. DESCRIPTIVE NOTES (Type of report and inclusive dates)

Third Quarterly Report - 15 June 1966 - 14 August 1966

5. AUTHOR(S) (Last name, first name, initial)

Lyon, John A. M., Alexopoulos, Nicholas G., Cha, Alan G., Digenis, Constantine J., and Parker, William W.

6. REPORT DATE	7a. TOTAL NO. OF PAGES	7b. NO. OF REFS
August 1966	58	5

8a. CONTRACT OR GRANT NO.	9a. ORIGINATOR'S REPORT NUMBER(S)
AF 33(615)-3371 b. PROJECT NO 4357 c. 435709 d.	7692-3-Q 9b. OTHER REPORT NO(S) (Any other numbers that may be assigned this report)

10. AVAILABILITY/LIMITATION NOTICES Qualified requestors may obtain copies of this report from DDC. This document is subject to special export controls and each transmittal to foreign governments or foreign nationals may be made only with prior approval of AFAL(AVPT, Wright-Patterson AFB, Ohio.

11. SUPPLEMENTARY NOTES	12. SPONSORING MILITARY ACTIVITY
	Air Force Avionics Laboratory AVWE Research and Technology Division, AFSC Wright-Patterson AFB, Ohio 45433

13. ABSTRACT

During this report period, additional studies were made on horns and slots surrounded by absorbing material. New designs were used which permitted all of the flush mounting material to be flush with the conducting surface. Swept frequency methods were used in obtaining values for the increased isolation over a considerable range of frequency.

Studies were made on the isolation of two antennas through the use of chokes. A slot antenna was constructed surrounded by four chokes in the form of circumferential trenches. For two systems, each equipped with such circumferential chokes, an additional 22 db of isolation was obtained.

Additional studies were made on the use of corrugations to increase isolations. The corrugations described here are not of an optimized design and do not use absorber material as has been planned for the future.

The use of simple parasitic antenna elements, such as slots as reflectors, has been used to improve system isolation. The improvement is rather small, being limited to about 7 db.

Considerable effort has been utilized on developing an RF bridge to improve isolation by cancellation of the unwanted signal. Results have been encouraging but work remains to adapt this method to a wider bandwidth.

DD FORM 1 JAN 64 1473

UNCLASSIFIED

Security Classification

14. KEY WORDS	LINK A		LINK B		LINK C	
	ROLE	WT	ROLE	WT	ROLE	WT
Coupling Decoupling Isolation increase						

INSTRUCTIONS

1. ORIGINATING ACTIVITY: Enter the name and address of the contractor, subcontractor, grantee, Department of Defense activity or other organization *(corporate author)* issuing the report.

2*a*. REPORT SECURITY CLASSIFICATION: Enter the overall security classification of the report. Indicate whether "Restricted Data" is included. Marking is to be in accordance with appropriate security regulations.

2*b*. GROUP: Automatic downgrading is specified in DoD Directive 5200.10 and Armed Forces Industrial Manual. Enter the group number. Also, when applicable, show that optional markings have been used for Group 3 and Group 4 as authorized.

3. REPORT TITLE: Enter the complete report title in all capital letters. Titles in all cases should be unclassified. If a meaningful title cannot be selected without classification, show title classification in all capitals in parenthesis immediately following the title.

4. DESCRIPTIVE NOTES: If appropriate, enter the type of report, e.g., interim, progress, summary, annual, or final. Give the inclusive dates when a specific reporting period is covered.

5. AUTHOR(S): Enter the name(s) of author(s) as shown on or in the report. Enter last name, first name, middle initial. If military, show rank and branch of service. The name of the principal author is an absolute minimum requirement.

6. REPORT DATE: Enter the date of the report as day, month, year; or month, year. If more than one date appears on the report, use date of publication.

7*a*. TOTAL NUMBER OF PAGES: The total page count should follow normal pagination procedures, i.e., enter the number of pages containing information.

7*b*. NUMBER OF REFERENCES: Enter the total number of references cited in the report.

8*a*. CONTRACT OR GRANT NUMBER: If appropriate, enter the applicable number of the contract or grant under which the report was written.

8*b*, 8*c*, & 8*d*. PROJECT NUMBER: Enter the appropriate military department identification, such as project number, subproject number, system numbers, task number, etc.

9*a*. ORIGINATOR'S REPORT NUMBER(S): Enter the official report number by which the document will be identified and controlled by the originating activity. This number must be unique to this report.

9*b*. OTHER REPORT NUMBER(S): If the report has been assigned any other report numbers *(either by the originator or by the sponsor)*, also enter this number(s).

10. AVAILABILITY/LIMITATION NOTICES: Enter any limitations on further dissemination of the report, other than those imposed by security classification, using standard statements such as:

(1) "Qualified requesters may obtain copies of this report from DDC."

(2) "Foreign announcement and dissemination of this report by DDC is not authorized."

(3) "U. S. Government agencies may obtain copies of this report directly from DDC. Other qualified DDC users shall request through _____."

(4) "U. S. military agencies may obtain copies of this report directly from DDC. Other qualified users shall request through _____."

(5) "All distribution of this report is controlled. Qualified DDC users shall request through _____."

If the report has been furnished to the Office of Technical Services, Department of Commerce, for sale to the public, indicate this fact and enter the price, if known.

11. SUPPLEMENTARY NOTES: Use for additional explanatory notes.

12. SPONSORING MILITARY ACTIVITY: Enter the name of the departmental project office or laboratory sponsoring *(paying for)* the research and development. Include address.

13. ABSTRACT: Enter an abstract giving a brief and factual summary of the document indicative of the report, even though it may also appear elsewhere in the body of the technical report. If additional space is required, a continuation sheet shall be attached.

It is highly desirable that the abstract of classified reports be unclassified. Each paragraph of the abstract shall end with an indication of the military security classification of the information in the paragraph, represented as *(TS), (S), (C), or (U)*.

There is no limitation on the length of the abstract. However, the suggested length is from 150 to 225 words.

14. KEY WORDS: Key words are technically meaningful terms or short phrases that characterize a report and may be used as index entries for cataloging the report. Key words must be selected so that no security classification is required. Identifiers, such as equipment model designation, trade name, military project code name, geographic location, may be used as key words but will be followed by an indication of technical context. The assignment of links, rules, and weights is optional.